ADDITIVE MANUFACTURING OF RF ABSORBERS

by

Matthew S. Mills

A thesis submitted to the Faculty of the University of Delaware in partial fulfillment of the requirements for the degree of Master of Science in Electrical and Computer Engineering

Winter 2016

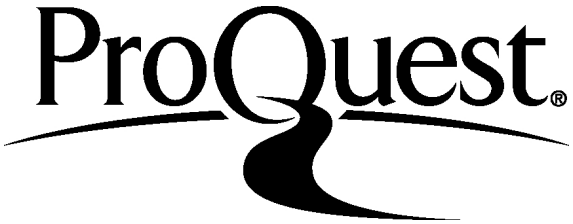

ADDITIVE MANUFACTURING OF RF ABSORBERS

by

Matthew S. Mills

Approved: _____
Mark S. Mirotznik, Ph.D.
Professor in charge of thesis on behalf of the Advisory Committee

Approved: _____
Kenneth E. Barner, Ph.D.
Chair of the Department of Electrical and Computer Engineering

Approved: _____
Babatunde A. Ogunnaike, Ph.D.
Dean of the College of Engineering

Approved: _____
Ann L. Ardis, Ph.D.
Interim Vice Provost for Graduate and Professional Education

ACKNOWLEDGMENTS

First, I would like to thank my advisors, Profs. Mark Mirotznik, for his direction, support, and guidance while conducting this research. I would also like to thank my colleagues, Pete, Zach, Paul, and Austin, for their encouragement, support, and laughter that helped make a fun and productive work environment.

I would like to specifically thank Zach and Peter; Zach provided the knowledge and experience required to produce fantastic nScrypt printed samples that helped make this research possible, and Peter provided me with the necessary training of measurement devices and modeling tools to allow me to complete this research effectively. I would also like to thank Sidd, Nick, and Eric for providing me with assistance through measurement and screen printing.

Lastly, I would like to dedicate this thesis to my wife for her daily support and encouragement that made it possible for me to get to where I am.

TABLE OF CONTENTS

LIST OF TABLES

LIST OF FIGURES

ABSTRACT

The ability of additive manufacturing techniques to fabricate integrated electromagnetic absorbers tuned for specific radio frequency bands within structural composites allows for unique combinations of mechanical and electromagnetic properties. These composites and films can be used for RF shielding of sensitive electromagnetic components through in-plane and out-of-plane RF absorption.

Structural composites are a common building block of many commercial platforms. These platforms may be placed in situations in which there is a need for embedded RF absorbing properties along with structural properties. Instead of adding radar absorbing treatments to the external surface of existing structures, which adds increased size, weight and cost; it could prove to be advantageous to integrate the microwave absorbing properties directly into the composite during the fabrication process. In this thesis, a method based on additive manufacturing techniques of composites structures with prescribed electromagnetic loss, within the frequency range 1 to 26GHz, is presented. This method utilizes screen printing and nScrypt micro dispensing to pattern a carbon based ink onto low loss substrates. The materials chosen for this study will be presented, and the fabrication technique that these materials went through to create RF absorbing structures will be described. The calibration methods used, the modeling of the RF structures, and the applications in which this technology can be utilized will also be presented.

Chapter 1

INTRODUCTION

Additive manufacturing is a growing field that when combined with practical electromagnetic designing constraints, may be utilized to fabricate electromagnetic structures that could not otherwise be created. The goal of this research project is to determine a method or methods which can be utilized to integrate electromagnetic absorbing characteristics within structural composites.

Through additive manufacturing techniques, patterned electromagnetic absorbers can be integrated within fabricated structures. The desired absorbing pattern may be deposited upon a specific substrate and measured to create ideal absorption characteristics. By adding these materials to fabric sheets or embedding them within a substrate, it is possible to combine desired electromagnetic properties with mechanical functionality to create multifunctional composite structures [1-4]. This research primarily focused on two different additive manufacturing techniques to deposit absorptive electromagnetic properties onto composite substrates. Namely; (1) nScrypt micro dispensing and (2) screen printing. These two different manufacturing techniques allow for both high resolution fabrication in the case of the nScrypt and large scale mass production in the case of screen printing.

1.1 Electromagnetic Absorbers

Electromagnetic absorbers are passive structures designed specifically to minimize the reflection and transmission of electromagnetic radiation. To accomplish

this engineers combine geometrical patterns of lossy dielectric and magnetic materials. Depending on the specific geometric design and materials used a broad range of electromagnetic absorbing technology have evolved [5-20].

The various absorber designs can be generally categorized into two types; (1) resonant narrow band absorbers and (2) broadband absorbers. The resonant absorber are designed to have large EM absorption over specific frequency bands. Common types of resonant absorbers include Salisbury screens, Jaumann absorbers, Dallenbach layer absorbers and circuit analog absorbers. More recently a new class of metamaterial based absorbers have been introduced. Figure 1.1 illustrates the geometry and materials used in these various resonant absorber methods.

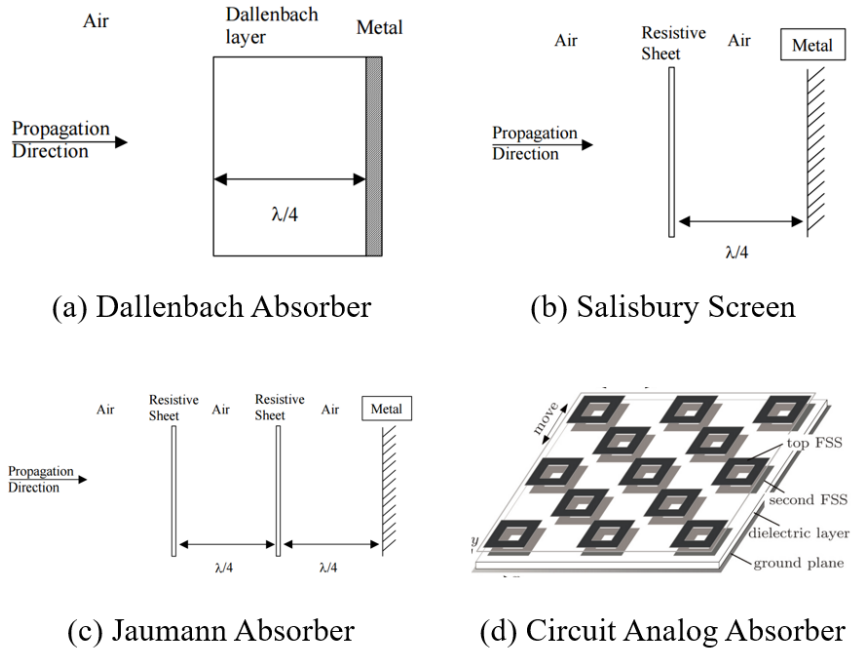

(a) Dallenbach Absorber (b) Salisbury Screen

(c) Jaumann Absorber (d) Circuit Analog Absorber

Figure 1.1 Illustration of various common methods to design resonant EM absorbers.

To realize non-resonant or broadband absorbers one needs to use other design methodologies. The most common technique is to grade the EM loss, or complex impedance Z, from the incident region (e.g. air) to a metallic ground plane. If the impedance taper is designed properly very wideband absorption can result. Figure 1.2 illustrates both continuous and discrete impedance tapers used to design broadband absorbers.

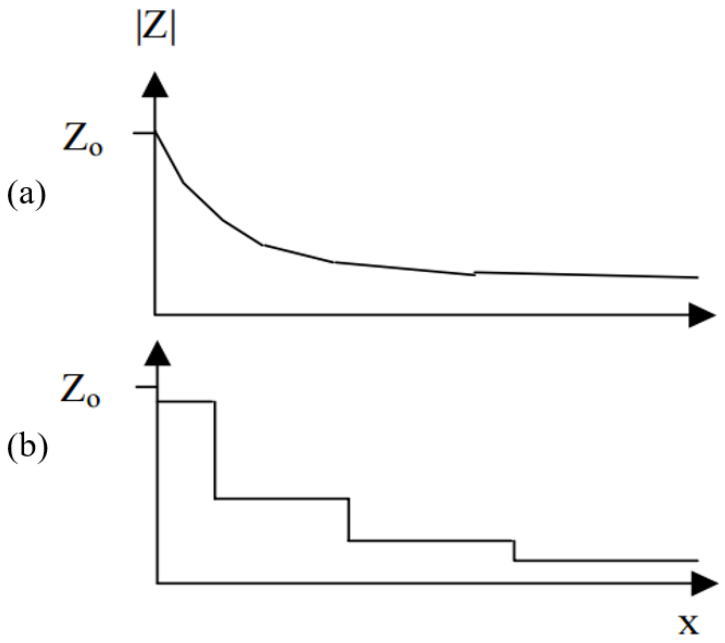

Figure 1.2 Continuous (a) and discrete (b) impedance tapers used to realize broadband absorbers.

Another class of absorbers are surface wave absorbers. The goal here is to attenuate surface waves that may be excited along a ground plane. There are a number of practical applications of this class of absorber including antenna design, reduction in

edge diffraction and minimizing cosite interference. Figure 1.3 illustrates a discretely graded surface wave absorber.

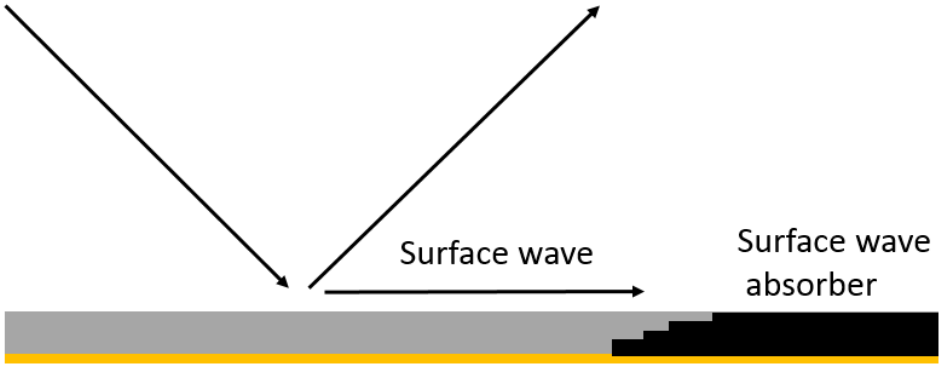

Figure 1.3 Illustration of surface wave absorber.

Fabrication of the various electromagnetic absorbers can be challenging. More advanced designs can require complicated 3D spatial variation of various materials. This is especially true when attempting to apply radar absorbing material to curved surfaces. One attractive new technology for EM absorber fabrication is the use of additive manufacturing (AM).

1.2 Additive Manufacturing

Currently, there are many methods that can be utilized to create RF absorbers [5-27]. The fabrication technique that was used in this research was additive manufacturing. Additive manufacturing is achieved through adding materials to an existing structure, or by creating a completely new structure by depositing new material onto a surface. The additive manufacturing techniques that were utilized in this research consisted of screen printing and nScrypt microdispensing.

Screen printing is a printing process that deposits a predetermined pattern onto a substrate material and is able to be repeated onto subsequent substrates. The process of screen printing is desirable due to its repeatability and its ability to produce results in minutes. nScrypt microdispensing is a printing process that is capable of accurately depositing materials through microdispensing heads in order to print a three dimensional structure. The microdispensing process, as compared to screen printing, is a highly accurate but time consuming process that is utilized to produce small scale precise samples. Both of these processes were used in the fabrication of RF absorbers and aided in the characterization of the carbon based ink and patterns that were utilized.

1.3 Thesis Outline

In Chapter 2, a materials section is discussed to describe the carbon based inks and substrates that were used in the fabrication of RF absorbers. In Chapter 3, the fabrication methods of screen printing and nScrypt micro dispensing are discussed and described in detail, along with the calibration process that was needed for both methods. In Chapter 4, the measurement and characterization of samples is described in detail. In Chapter 5, the numerical modeling and the methods for backing out the DuPont 7082 properties are discussed. To conclude, Chapter 6 will discuss the conclusions and the future work that can be done in the design and fabricating of in-plane and out-of-plane RF absorbers.

Chapter 2

MATERIAL SELECTION

In this chapter, I will discuss the material selection process that was necessary in order to create RF absorbing properties. The selection process required that two primary materials needed to be determined in order to create these absorbers. The first material that needed to be selected was a printable ink that could sustain a high loss tangent. The ink had to be compatible with screen printing and microdispensing processes and facilitate desirable electromagnetic properties. The second material that needed to be selected was the substrate to be printed upon. The substrate needed to be compatible with the fabrication processes, have the ability to withstand the curing temperatures of the selected ink, and needed to have a low permittivity.

2.1 Ink Selection

The additive manufacturing techniques that were utilized in this research required that an ink be deposited onto or within a substrate. The ink that was to be selected needed to be able to produce desirable attenuation over a specific frequency range. The frequency range that was used in determining the attenuation of the inks was within the 18 to 26GHz range.

Carbonaceous particles were selected as the loss material to be suspended in an ink or resin. They can be used to tailor the absorption properties of the deposited material in order to modify the absorptive properties of the substrate in which they are deposited[1]. In order for the ink to provide enough attenuation within the desired frequency range, a selection process of the carbonaceous particles and ink need to be completed. The carbonaceous particle type that was selected for this research was carbon black.

In an attempt to create in-house high loss inks, Regal 400R Carbon black particles were obtained from Cabot Corporation to test sheer mixing varying amounts of carbon black particles with a plastisol ink. International Coatings 10 NP Clear Multi-Purpose Plastisol Ink and Atlas Screen-Supply Company Plastisol Ink Curable Reducer were used in an attempt to create an in house screen printable high loss ink. These mixed inks were determined to be non-usable, due to the fact that the viscosity was beyond the applications of the screen printer. Once it was determined that making inks in-house was not a worthwhile endeavor, multiple commercial inks were tested in order to determine an ink with ideal printing and absorption characteristics. BARE Electric Paint, YSHIELD HSF54, and DuPont 7082 Resistor Ink were used in an attempt to determine an ideal ink for printing. The inks were tested by hand rolling a layer of the different inks onto a Kapton film. The samples were then measured in an anechoic chamber and the transmission data was recorded. The DuPont 7082 Resistor Ink was determined to be the desired ink. The BARE and YSHIELD both provided too much reflection, whereas the DuPont ink absorbed a portion of the transmission.

There was one other ink selection process that was necessary to this research. In order for the nScrypt to create a sample that could be used to create in-plane absorbing samples of the DuPont 7082, a conductive ink needed to be selected. The conductor that was used in this research was a printed trace using DuPont CB028 silver conductor paste. DuPont CB028 has been determined to have a conductivity of 1×10^7 S/m [3].

2.2 Substrates

In order to create a structural composite out of the screen printed material, the proper substrate needed to be selected. The substrate needed to have a low loss tangent and a low permittivity. The substrates that were selected and print tested were 6781 s-

glass 8HS 8oz, Honeywell Spectra Shield 2 SR-3124, DuPont 2mil Kapton film, and Matter Hackers polycarbonate filament. The first three substrates all printed well through screen printing, and nScrypt micro dispensing; however, Kapton was best for nScrypt micro dispensing due to the surface being consistent and there were no loose fibers. The nScrypt was also used printed a polycarbonate filament that was used as the substrate to create transmission line to create in-plane absorbers.

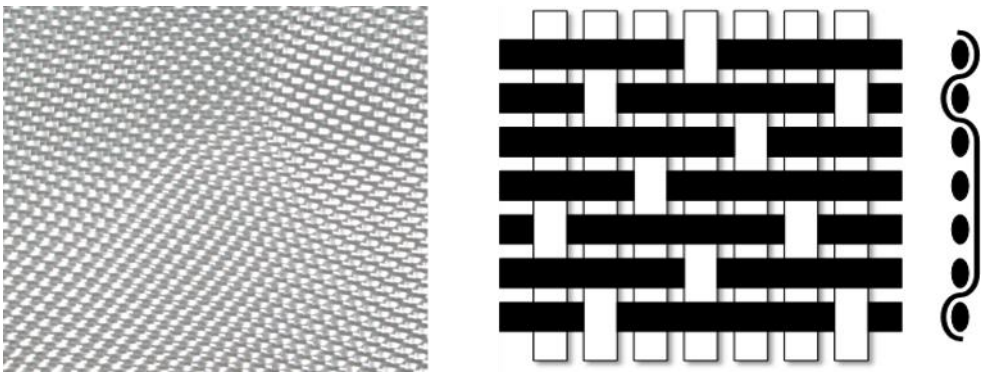

Figure 2.1 6781 8HS 8oz s-glass (pictured left) and satin weave fabric (pictured right).

The s-glass that was chosen is a woven glass fabric. This fabric can be manipulated to form a desired shape and infused with resin to make it into a structural composite, s-glass pictured in Fig. 2.1. Through careful alignment and applying modifications to the screen printer, a roll-to-roll printing system was created. The roll-to-roll system allowed for a high amount of throughput with consistent printing. This allowed the screen printing system to constantly print onto the s-glass, and once printing was complete, the pattern could then be cut to the necessary size and utilized as needed. The drawbacks to screen printing onto s-glass fabric is that the woven fabric has hills

and valleys, which create a polarization dependence of the printed sample, which can vary from sample to sample; also, nScrypt micro dispensing can be difficult to print onto s-glass due to glass fibers being pulled up into the dispensing head.

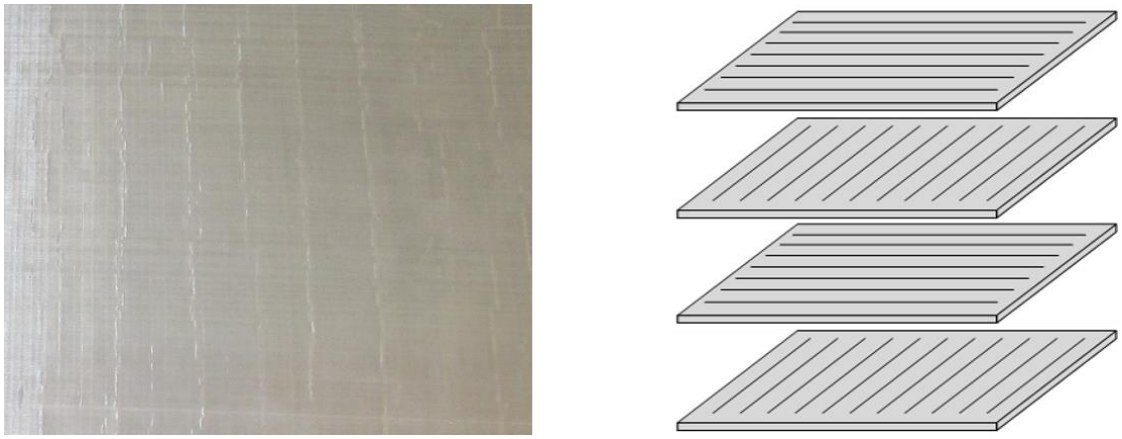

Figure 2.2 Honeywell Spectra Shield 2 SR-3124 (pictured left) and an example of the unidirectional layers that stack to create the substrate (pictured right).

Spectra Shield, as seen in Fig. 2.2, is a made of sheets of unidirectional polyethylene fibers that are stacked on top of one another to create a ballistic composite material that is primarily used in armor applications. The goal of using spectra shield as a substrate was to show that RF absorbing characteristics could be incorporated with ballistic composite sheets. The spectra shield was primarily used as a substrate for screen printing. Through screen printing patterns of DuPont 7082 onto the substrate, RF absorbing characteristics were added to the substrate. This allows for RF absorbing characteristics to be implemented where armor applications could be utilized. The drawback to printing onto Spectra Shield is that the polymer fibers are in one direction, and this caused a slight issue with screen printing, because the screen printer needed to

print in the direction of the fibers. There was also a slight polarization dependence of each sample; nScrypt micro dispensing can be difficult to print onto Spectra Shield due to the polymer fibers being pulled up into the dispensing head.

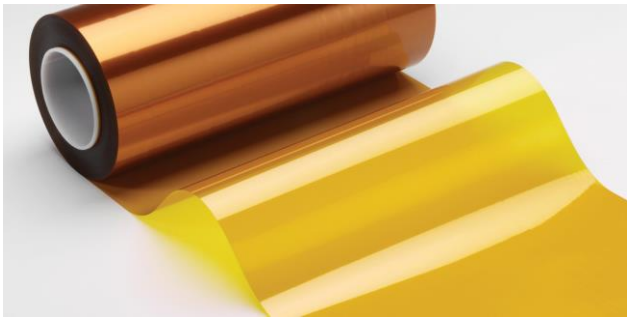

Figure 2.3 DuPont 2mil Kapton film.

Kapton, as seen in Fig. 2.3, is a polyimide film that has high flexibility and is resistance to temperatures up to 400°C. Kapton is also able to be printed upon and embedded within a structural composite [3-4]. The goal of printing onto Kapton film was to aid in the characterization of the selected ink. Kapton was a desirable substrate for characterization because it has a consistent surface thickness and low loss tangent. The consistent thickness allowed for even deposition of ink through nScrypt micro dispensing. The substrate was suitable for screen printing techniques; however, it was not pursued because the material was not accepting of multiple print layers.

Chapter 3

FABRICATION METHODS

In this chapter, I will discuss the fabrication methods that were utilized to couple RF absorbing properties with structural composites. Since the focus of this research was to utilize additive manufacturing techniques to couple RF absorbing properties, the processes needed to be compatible with the composite substrates. The methods of additive manufacturing that were used to conduct this research were screen printing and nScrypt micro dispensing. Through using these tools to create RF absorbers, a reliable and repeatable process needed to be created and followed in order to create samples. The processes of screen printing and nScrypt microdispensing will be discussed, and modifications to the standard procedures will be shown.

3.1 Screen Printing

Screen printing is a process of additive manufacturing that utilizes a mesh screen, a flood, and a squeegee, as seen in Fig. 3.1. The mesh screen that is used will contain a desired pattern that will be deposited onto the substrate. When the flood is actuated, it will deposit ink across the surface of the screen, the screen is then lowered to a snap-off height above the substrate, and then the squeegee actuates to deposit the desired pattern onto the substrate. The substrate is then heated to cure the deposited ink. This process allows for a designed pattern to be repeatedly deposited onto multiple substrates in a short period of time. Which makes the screen printing process appealing for mass fabrication of repeated designs that need to be deposited onto multiple substrates.

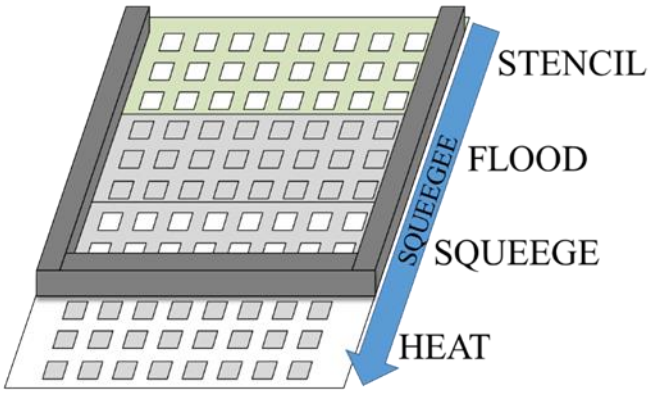

Figure 3.1 Flow of screen printing process

The screen printer used in this research was a Grafica Flextronica Nano-Print Plus model number GF-2228-N.P.P, pictured in Fig. 3.2. Screens were designed using Rhino CAD and purchased from UTZ manufacturing. The screen frames used were 29 inch by 29 inch frames with a non-inset screen. The screen had a 28.5 degree stretch angle with a 325 mesh that had a width of .0011 inches and a 0.001 inch emulsion thickness. The screen printer itself has adjustments to fit screens of multiple sizes and the capability of incorporating multiple snap-off heights. The screen printer utilized a standard squeegee and flood bar, which were attached to an actuating motor. The flood and squeegee have fine adjustments that allow the user to adjust the position of the flood or squeegee. The screen printer has settings to flood, squeegee, lower the screen, and raise the screen. The squeegee and flood have a speed adjustment to allow for a slower snap-off.

Figure 3.2 Grafica Flextronica Nano-Print Plus.

3.1.1 Screen Printing Modifications

Through experimentation and design, the screen printer required a few modifications in order to properly deposit the desired patterns reliably. The first modification that was needed was to modify the squeegee, pictured in Fig. 3.3. The squeegee of a screen printer is made of a chemical resistive polymer that is held in place by a clamp. In order to seat the squeegee properly, the squeegee bar needed set screws to be inserted to apply equal pressure across the squeegee so that the print edge of the squeegee was flush with the surface of the screen. The second necessary modification was to create a heat box that could provide a surface cure to the printed inks, pictured in Fig. 3.3. The design of the heat box was necessary due to the fact that if heat was applied without it, the heat would rise to the screen and cure the ink in the mesh of the screen. By creating the heat box, the heat was able to be applied directly where needed.

The third and final modification to the screen printer was to incorporate a roll-to-roll system, pictured in Fig. 3.3. This system was implemented by attaching a rolling bar to the front and back of the screen printer. The roller was tested and successfully printed a sixteen foot section of continuous printed substrate. These modifications allowed for a more reliable and repeatable screen printing process.

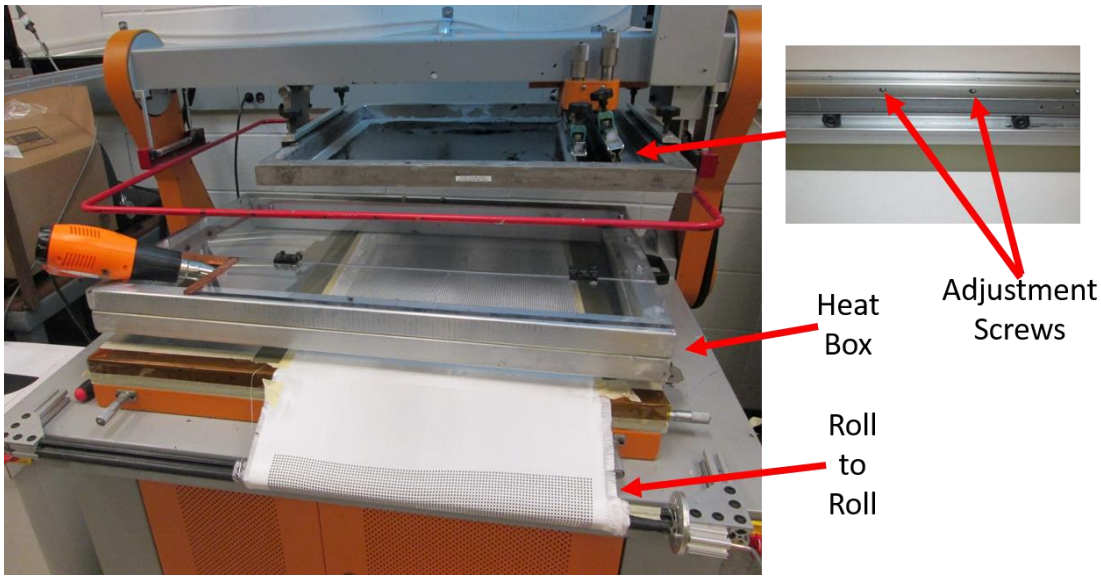

Figure 3.3 Screen printer modifications.

3.1.2 Out of Plane Absorbers

The samples that were created through screen printing were fabricated using screens that were designed with a periodic pattern. The pattern chosen was a square patch pattern, and the size of the patch was varied while the period remained constant, pictured in Fig. 3.4. The patch size of the periodic pattern could be varied from .5 to 4mm, depending on the screen used, and the period was kept constant at 4mm; this allowed for varying the amount of ink deposited while maintaining a repeating pattern.

The screen printed substrates, spectra shield and s-glass, were printed with a double pass function of the printer. Three double passes were applied to the substrates, and a surface heating was applied between each of the three passes. The surface heating allowed for a buildup of ink to be deposited onto the substrate. Upon completion of screen printing, the samples were cured in a convection oven at 120 C for 30 minutes. This allowed for a thorough cure of the DuPont 7082 and outgassing of the polymer that was used to bind the particles. The varying print patterns allowed for the amount of attenuation to also be varied between the different patterns. However, due to the screen printer depositing ink in one direction, there was a slight elongating of the printed patch. The elongation of the printed pattern and the fiber pattern of the substrate created a polarization difference from sample to sample, this is seen and discussed in the results section of chapter 4.

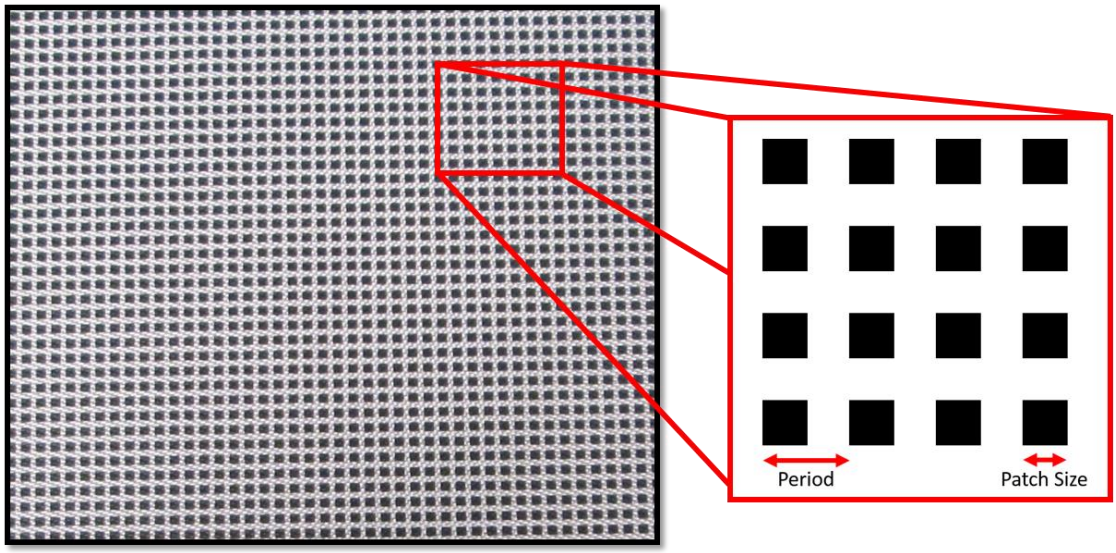

Figure 3.4 Screen printed pattern deposited onto s-glass.

3.2 nScrypt Microdispensing

Micro dispensing is a process of additive manufacturing that utilizes a dispensing head to precisely deposit a material. The micro dispensing system that was used in this research was a nScrypt 3Dn-300, pictured in Fig. 3.5. The system is capable of utilizing two different types of dispensing heads for depositing a wide variety of materials. The implementation of two print heads allows for the printing system to toggle between printing two materials at the same time. These materials may also be swapped out mid print in order to incorporate varying properties within one structure.

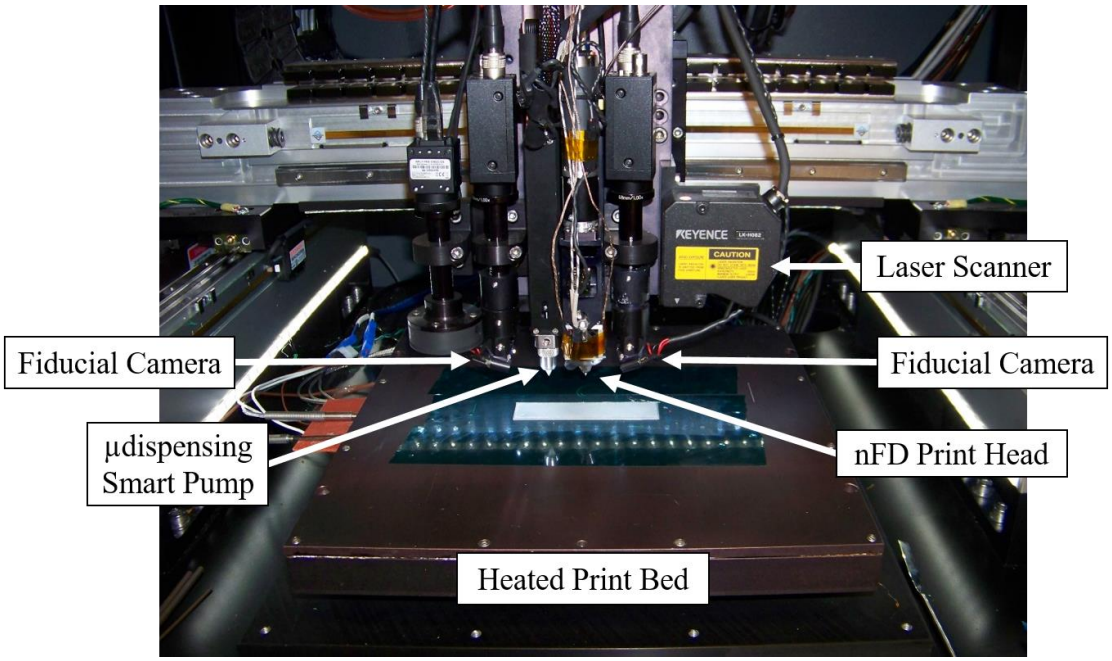

Figure 3.5 nScrypt 3Dn 300.

The first dispensing head is a micro dispensing smart pump that utilizes pneumatic pressure to extrude material from a syringe to a dispensing tip at a constant rate. The second dispensing head is an nFD print head that is used to print thermal

plastics. Both print heads are capable of producing 25µm lines at a rate of 300mm/s and the stages have positional accuracy up to 1µm. The nScrypt is also equipped with a laser scanner that allows the user to scan a surface, so that the nScrypt can provide a constant print on a curved surface. The ability to scan a part and calibrate to any surface allows for precise deposition of material onto most substrates. The nScrypt also has the ability to vary the pressure and valve opening of the smart pump, which allows the micro dispensing extrusion process to print a wide variety of viscosities varying from 0-1,000,000 cps. The smart pump was used for the deposition of DuPont 7082 Resistor Paste and DuPont CB028 Silver Conductive Ink, and the nFD print head was used to print polycarbonate thermal plastic.

During this research, the nScrypt was utilized to print two types of samples. These samples were created through utilizing the micro dispensing smart pump and the nFD. In order to deposit the desired structures, the print pattern is first designed as a 3D model and saved as a single thickness layer file. That file is then converted to readable g-code, which is the code that is used by the nScrypt, and printed by the nScrypt.

3.2.1 Out of Plane Absorber

The first set of samples that were fabricated with the nScrypt used the smart pump to print DuPont 7082 onto Kapton film. These samples were designed to vary the period of the DuPont 7082 being deposited onto the Kapton film, pictured in Fig. 3.6. The period of these samples were varied from 500µm, 700µm, and 900µm. The line thickness of these samples was approximately 25µm. And the line width of these samples was approximately 310µm. The dimensions of these samples were measured and are discussed in chapter 4. Once printing is complete, the samples are placed in a

convection oven at 120 C for 30 minutes to allow for a thorough cure of the ink. By varying the line spaces of these samples an analysis method, discussed in chapter 5, can be used to back out the material properties of the DuPont 7082.

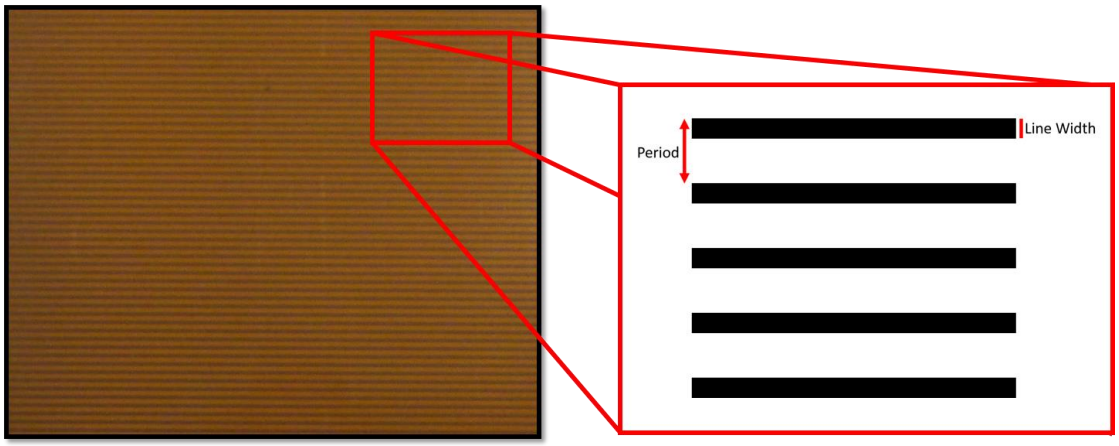

Figure 3.6 Print pattern of Kapton film.

3.2.2 In-Plane Absorber

The nScrypt was used in the creation of in-plane absorbers. The smart pump and nFD print heads were necessary in the creation of these samples. The creation of these samples was accomplished by printing a substrate of polycarbonate that contained within it an inclusion of DuPont 7082. A microstrip transmission line was then printed on the top surface of the substrate, using DuPont CB028, to measure the properties of the substrate. In order to understand the behavior of the transmission line with no DuPont 7082, a baseline sample of polycarbonate was created. The substrate of this sample was printed using the nFD print head, and a microstrip trace was printed on the top surface using the smart pump to print the DuPont CB028. This sample is pictured

in Fig. 3.7. The sample had a width of 25mm, a substrate height of 1.2mm, a trace width of 3.1mm and a length of 100.75mm.

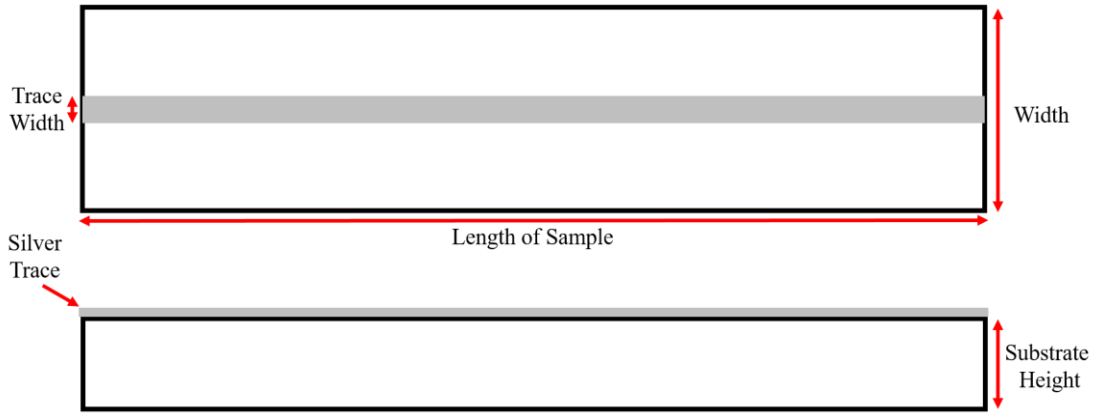

Figure 3.7 Baseline transmission line of polycarbonate, top view (top) and side view (bottom).

The first set of in-plane absorbing samples were fabricated by using the nFD print head to build up a polycarbonate substrate that contained a section that was absent of polycarbonate. This section was then filled by using the smart pump to deposit DuPont 7082 within the section. Once the DuPont 7082 was dispensed and cured, a capping layer of polycarbonate was added to the top of the sample. This effectively trapped the DuPont 7082 within the sample. DuPont CB028 was then printed on the top of the capping layer as the trace of the microstrip line, the layout of these samples can be seen in Fig. 3.8. There were four samples created using this method. The length, width, substrate height, length of inclusion, and trace width of these samples were kept constant at 100.75mm, 25mm, 1.2mm, 82mm, and 3.1mm respectively. The side profile of the samples are listed in Table 3.1. The measurement results of these samples are

discussed in chapter 4. By shifting the slab of DuPont to be off center, Distance A and Distance B are not equal, the loss associated with the substrate could be changed. It was noted that the loss was not one that followed a simple mixing law [15]. Through modeling, discussed in chapter 5, it was found that as the DuPont 7082 is placed closer to the surface of the substrate, the loss is increased. A new set of samples was fabricated to demonstrate the increase of loss.

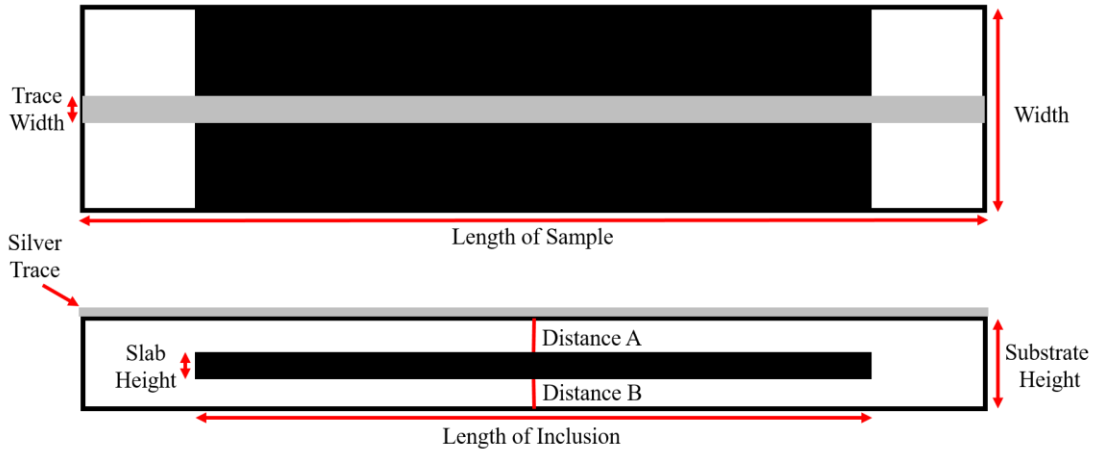

Figure 3.8 Transmission line with DuPont 7082 slab centered, top view (top) and side view (bottom).

Table 3.1 SIDE PROFILE DESCRIPTION OF IN-PLANE ABSORBER SAMPLE SET 1.

Sample	Slab Height	Distance A	Distance B
1	.15 mm	.3 mm	.75 mm
2	.3 mm	.45 mm	.45 mm
3	.45 mm	.3 mm	.45 mm
4	.6 mm	.3 mm	.3 mm

The second set of in-plane absorbing samples were fabricated in a similar manner to that of the first. These samples were created by using the nFD print head to build up a polycarbonate substrate that contained a section near the top of the substrate that was absent of polycarbonate. This section was then filled by using the smart pump to deposit DuPont 7082 within the section. Once the DuPont 7082 was dispensed and cured, DuPont CB028 was then printed on the top of the substrate as the trace of the microstrip line, the layout of these samples can be seen in Fig. 3.9. There were three samples created using this method. The length, width, substrate height, length of inclusion, and trace width of these samples were kept constant at 100.75mm, 25mm, 1.2mm, 25mm, and 3.1mm respectively. The slab height had the three values of .3mm, .6mm, and .9mm.

Figure 3.9 Transmission line with DuPont 7082 slab at top of substrate, top view (top) and side view (bottom).

Upon measurement and simulation of the varying structures printed within the polycarbonate substrate, a sample that incorporated a step grading of the DuPont 7082

was designed for optimal absorbing characteristics. This sample was printed in a similar manner to the samples in the second set of in-plane absorbers, but the sample used a step grading to increase the amount of DuPont 7082. Once the DuPont 7082 was dispensed and cured, DuPont CB028 was printed on the top surface of the substrate, the layout of this sample can be seen in Fig. 3.10. The length, width, substrate height, step length, and trace width of this sample was 100.75mm, 25mm, 1.2mm, 1.25mm, and 3.1mm respectively. The step height and length of inclusion can be seen in Fig. 3.11.

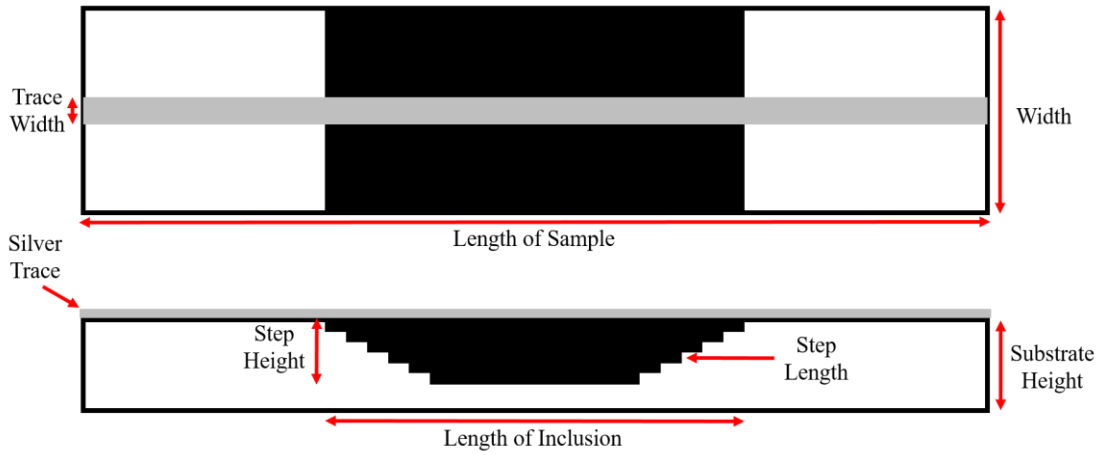

Figure 3.10 Transmission line with DuPont 7082 step slab at top of substrate, top view (top) and side view (bottom).

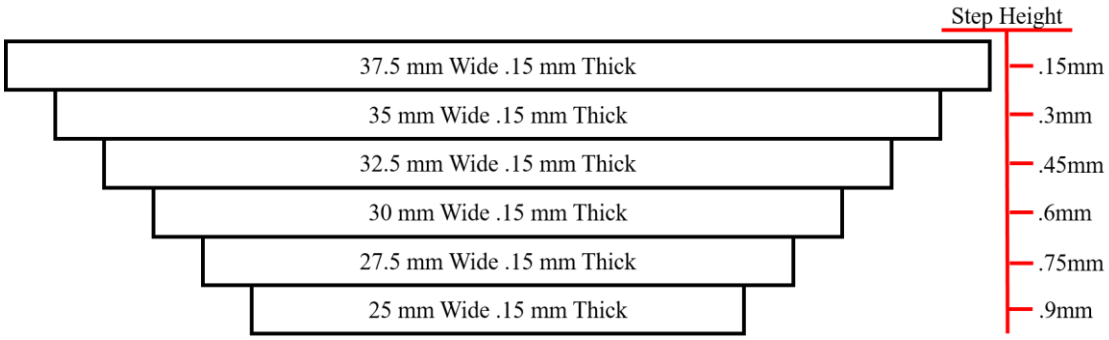

Figure 3.11 Step profile of DuPont 7082 within polycarbonate.

3.3 Fabrication Methods Conclusion

Samples were fabricated utilizing both screen printing and nScrypt microdispensing. Screen printing was primarily used to create large scale out of plane RF absorbers. This printing technique allows the user to combined RF absorption characteristics with structural composite sheets. nScrypt microdispensing was used in the fabrication of small scale in-plane and out of plane RF absorbers. Through this printing technique, samples were fabricated that utilized transmission line design to create in-plane absorbers and accurately deposited line structures to create out of plane absorbers that were used to characterize DuPont 7082. Pictures of fabricated samples can be seen pictured in Fig. 3.12.

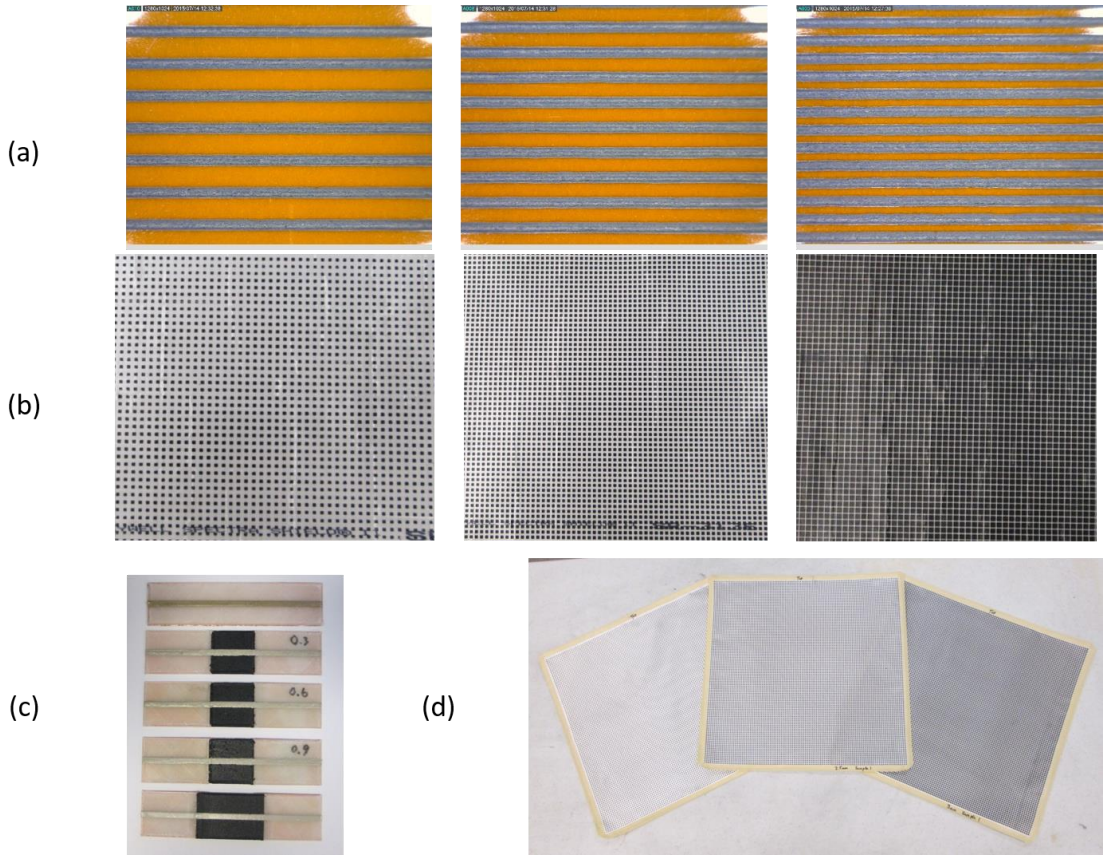

Figure 3.12 Example pictures of samples created through additive manufacturing techniques, samples are listed left to right and top down. (a) Kapton samples nScrypt printed, 900µm period, 700µm period, 500µm period; (b) spectra shield samples screen printed, 2mm patch, 2.5mm patch, 3.5mm patch; (c) transmission line samples nScrypt printed, baseline, .3mm thick slab, .6mm thick slab, .9mm thick slab, and optimized step slab; (d) s-glass samples screen printed, 2mm patch, 2.5mm patch, and 3mm patch.

Chapter 4

MEASUREMENT AND CHARACTERIZATION

In this chapter, I will discuss the electromagnetic measurement processes, the profile measurement process, and the results that were recorded. This process was necessary in order to aid in the characterization of the complex permittivity of the DuPont 7082. The measuring device that was used to measure the S parameters of the samples was an Agilent Technologies E8364B 10MHz – 50GHz Portable Network Analyzer. A Keyence VK-X200 laser microscope was used to take confocal measurements of the three dimensional profile of the Kapton nScrypt printed samples in order to better understand the structure and back out the complex permittivity of the DuPont 7082.

4.1 Measurement Setup

4.1.1 Out of -Plane Measurements

The out of plane measurements were recorded by collecting transmission data with the sample mounted in an anechoic chamber and recording the S12 data, this setup is pictured in Fig. 4.1. The sample was attached to a mount located in the center of the anechoic chamber. Two focused beam antennas were mounted onto linear motor stages, and were spaced with a 30 inch focal distance from the sample. The antennas were connected to the network analyzer and were calibrated using a THRU open air transmission. The data of the measured samples was recorded with both zero and ninety degree orientations.

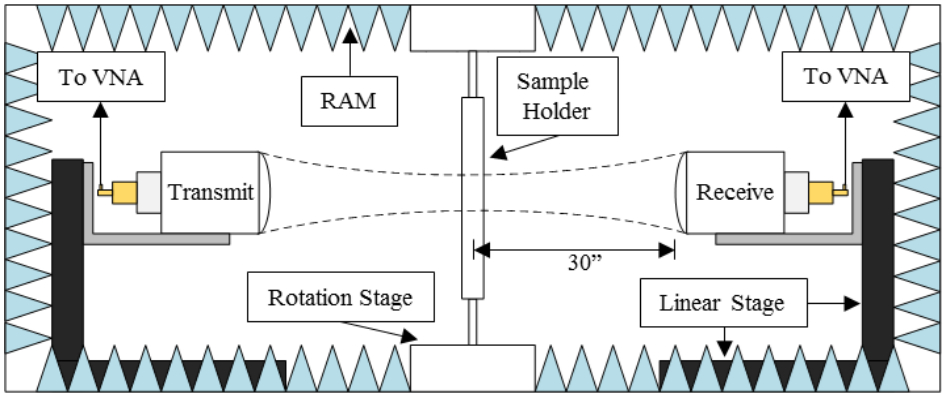

Figure 4.1 Focused beam measurement system within a radar absorbing anechoic chamber.

4.1.2 In-Plane Measurements

The in-plane S parameter measurements were recorded by collecting data from a microstrip transmission line. The transmission line was mounted onto a test fixture and connected via two test port cables to ports 1 and 2 of the network analyzer. The system was calibrated using an OPEN, SHORT, LOAD, and THRU calibration routine and Agilent 85052 D 3.5mm Economy Calibration Kit, the measurement setup is pictured in Fig. 4.2.

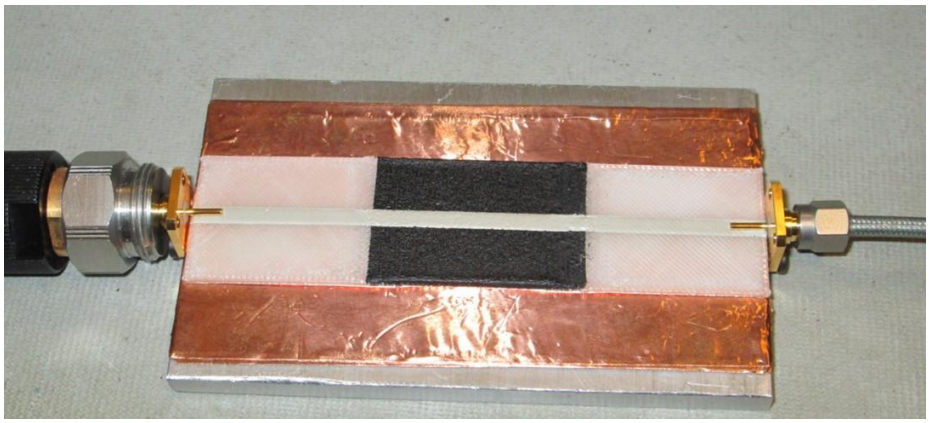

Figure 4.2 Transmission line fixture connected to VNA to measure S parameters.

4.1.3 Microstrip Transmission Line Design

A microstrip transmission line consists of a thin conducting strip that is placed above a dielectric substrate, which is supported on the bottom by a conducting ground plane, pictured in Fig.4.3. The microstrip transmission line is an evolution of the coaxial transmission line [28-30]. The design equation for the impedance of the transmission line are determined based on the substrate material, height of the substrate, and the width of the microstrip line.

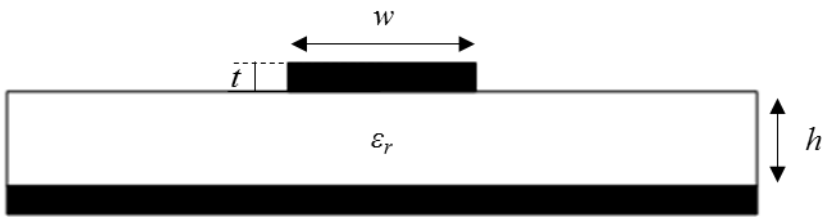

Figure 4.3 Microstrip transmission line.

The required equations to design the transmission line and calculate the input impedance are well known and discussed [28-30]. The miscrostip transmission line was designed and modeled in Ansys High Frequency Structure Simulator (HFSS). The transmission line was designed for a trace width of 3.1mm, a length of 100.75mm, a substrate width of 25mm, and a height of 1.2mm. The connector used were 50ohm SMA connectors attached to a fixture. The fixture allowed for transmission lines to be swapped out to take measurements for each sample. The strip like was printed DuPont CB028 and the ground plane was made using copper tape.

4.1.4 Imaging of Samples

In order to understand the profile of the samples and to back out the complex permittivity, measurement devices capable of measuring the printed profile needed to be utilized. The device that was used to measure the profile of the nScrypt printed Kapton samples was a Keyence VK-X200 laser microscope, pictures of the measured sample profile can be seen in Fig.4.4. This profile measurement technique was completed at five different locations on each sample and averaged out to find the best values. The confocal microscope was used to determine the surface profile of the pattern that was deposited onto the Kapton samples. The averaged measured profile of the samples are listed in Table 4.1. This profile data was utilized in the characterization of the complex permittivity of the DuPont 7082 ink, discussed in chapter 5. The profile of the 700μm period varied slightly from sample to sample, but by having the profile data, this variation was accounted for in the characterization process.

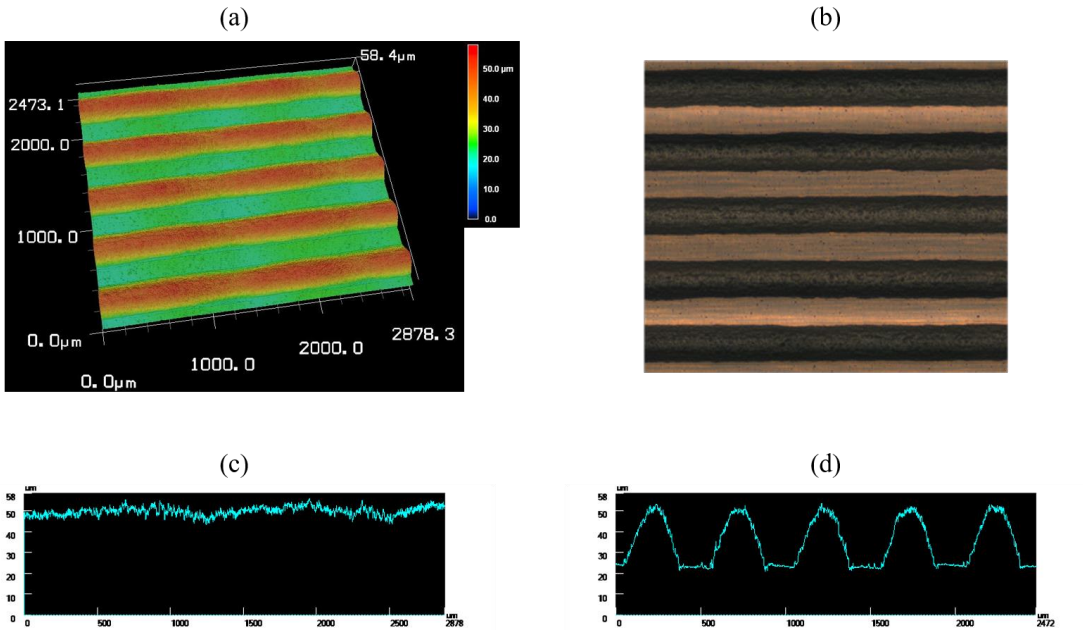

Figure 4.4 Confocal imaging of 500µm period nScrypt printed Kapton sample: (a) 3-D profile of sample; (b) optical image of sample; (c) horizontal profile of line; (d) profile of line width.

Table 4.1 PROFILE MEASUREMENTS OF NSCRYPT PRINTED KAPTON SAMPLES

Sample Number	Period (µm)	Line Height (µm)	Line Width (µm)
1	499	26.8	328
2	500.	25.8	300
3	498	26.4	314
4	703	22.8	255
5	700	22.4	280
6	702	25.4	310
7	902	22.8	315
8	903	24.0	310
9	900	22.8	315

4.2 Measured Results

4.2.1 S-Glass Results

The s-glass printed samples were measured using the out of plane measurement technique. The S12 results of the samples were grouped based on their print patterns and the orientation, zero and ninety degree, of the measurement. The s-glass samples were fabricated using the screen printing technique. Because of this, the orientations contained a different amount of material deposition in one direction than another, this is due to the weave and weft pattern of the substrate and the printing process of the screen printer. This change in material meant that more of the DuPont 7082 would interact with the electromagnetic wave in one orientation than another, which in turn caused a larger amount of attenuation associated with this direction. The screen printing process also allowed for a slight variation of the amount of DuPont 7082 deposited upon the substrate, and while the screen printing process is highly repeatable, the variation of pressure from sample to sample creates a slight variation in the amount of DuPont 7082 that is deposited upon the substrate. This variation in the DuPont 7082 created a slight shift of attenuation between samples that contain the same periodicity. Due to this error, a set of six samples was taken of four different print patterns and the average of these samples was taken and plotted, as seen below in Fig. 4.5. The plot shows the polarization dependence of the samples and also shows the shift in loss as the patch size is increased. The patch sizes chosen were based on the reliability of the screen printing process and the loss associated with the sample pattern. With the smaller patch sizes, it was difficult to reliably repeat the printed sample.

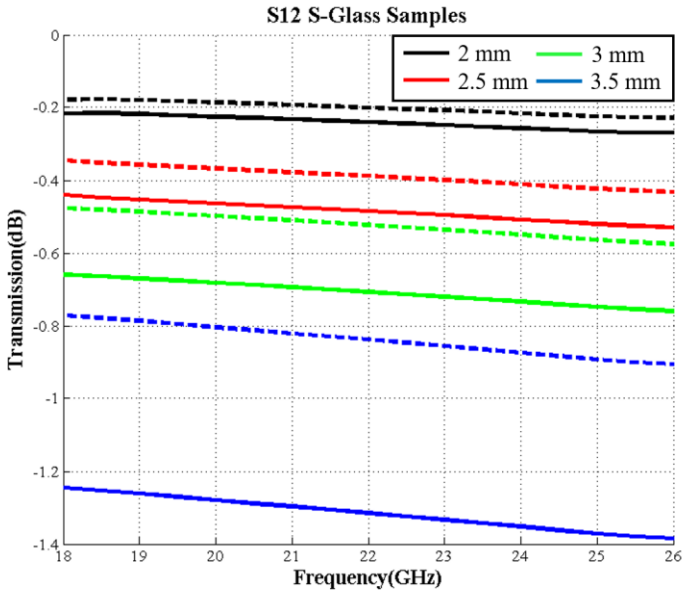

Figure 4.5 S-glass screen printed samples. The solid lines represent the ninety degree orientation and the dashed lines represents the zero degree orientation.

4.2.2 Spectra Shield Results

The spectra shield printed samples were measured utilizing the out of plane measurement technique. The S12 results of the samples were grouped based on their print patterns and the orientation of the measurement. The spectra shield samples were fabricated using screen printing techniques. The unidirectional fiber layers that make the spectra shield samples acts as more of a film, which helped in the material deposition process and only allowed for a minor shift between measurement polarizations. However, as was seen with the s-glass samples, the screen printing process allowed for the samples have a slight variation in the amount of DuPont 7082 that was deposited. This variation in the DuPont 7082 created a slight shift of attenuation between samples that contain the same periodicity. Due to this error, a set of four samples was taken of three different print patterns and the average of these samples was taken and plotted, as

seen below in Fig. 4.6. The plot shows that there is a very minor polarization dependence of the spectra shield samples and it also shows the shift in loss as the patch size is increased. As with the s-glass samples, the patch sizes chosen were based on the reliability of the screen printing process and in an attempt to maximize the loss associated with the sample pattern.

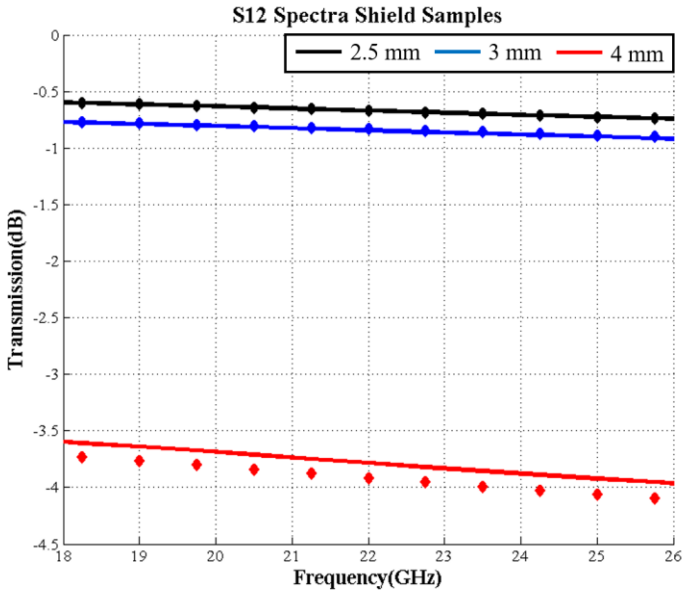

Figure 4.6 Spectra shield screen printed samples. The solid lines represent the ninety degree orientation and the diamond lines represents the zero degree orientation.

4.2.3 Kapton Results

The Kapton printed samples were measured utilizing the out of plane measurement technique. The S12 results of the samples were grouped based on their print patterns and the orientation of the measurement. The samples were fabricated by nScrypt microdispensing. As seen by the confocal images, the unidirectional printed

line patterns contained little variation from sample to sample. The variation in measured results were due minor fabrication errors that caused the lines of a few samples to be thinner or thicker than intended. The line width is primarily what caused the shift of the samples within the same sample set. The measurement data of the sample sets of the 500µm, 700µm, 900µm period can be seen in Fig. 4.7, Fig. 4.8, and Fig. 4.9.

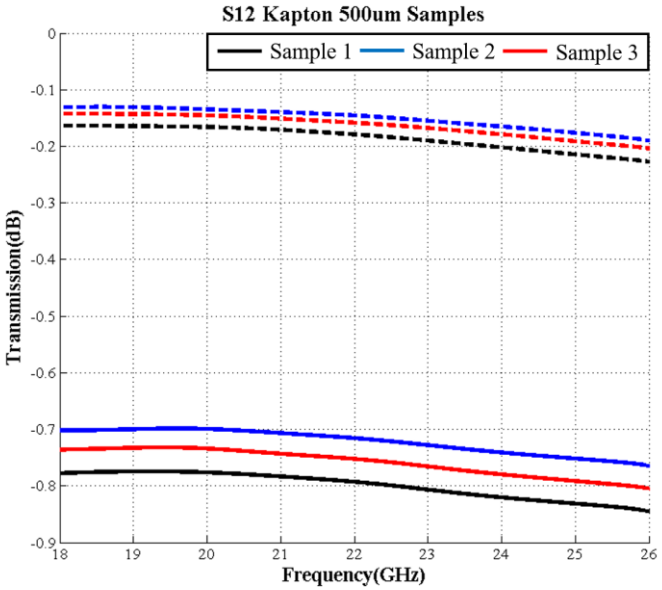

Figure 4.7 Kapton nScrypt printed 500µm samples. The solid lines represent the ninety degree orientation and the dashed lines represents the zero degree orientation. The shift from samples is due to the amount material deposited. This corresponds well with the measurements in Table 4.1.

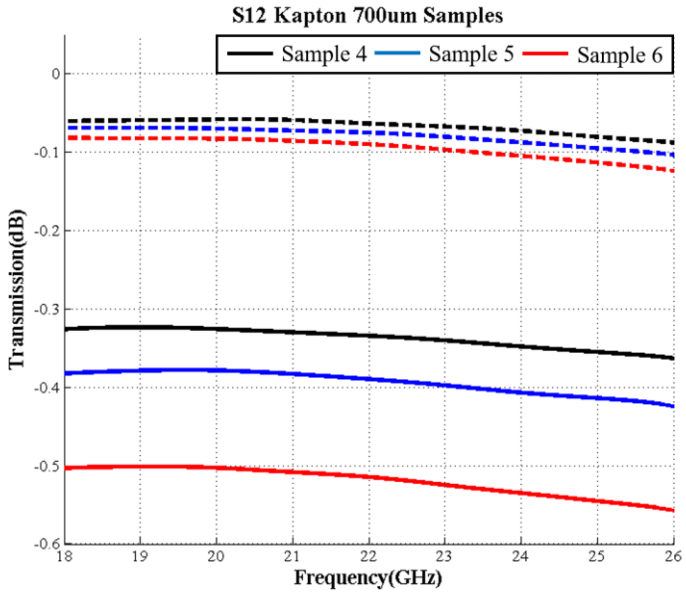

Figure 4.8 Kapton nScrypt printed 700µm samples. The solid lines represent the ninety degree orientation and the dashed lines represents the zero degree orientation. The shift from samples is due to the amount material deposited. This corresponds well with the measurements in Table 4.1.

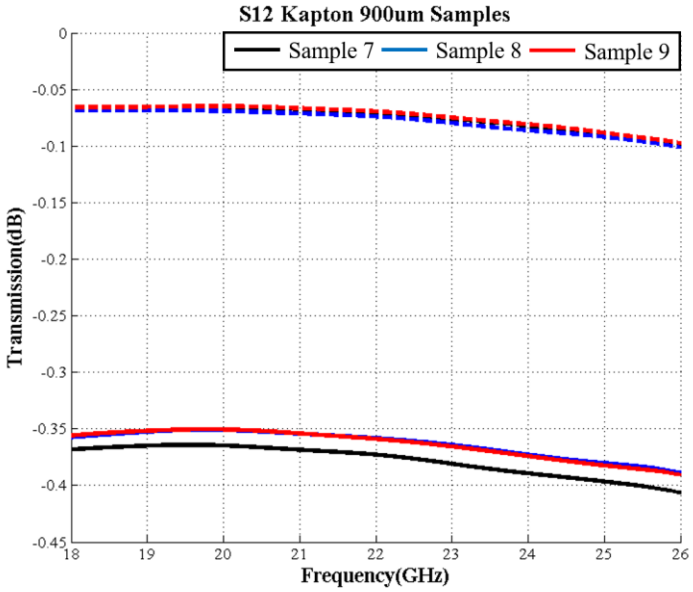

Figure 4.9 Kapton nScrypt printed 900µm samples. The solid lines represent the ninety degree orientation and the dashed lines represents the zero degree orientation. The zero and ninety degree orientations of these samples were very closely matched with one another. The minor shift from samples is due to the amount material deposited. This corresponds well with the measurements in Table 4.1.

4.2.4 Polycarbonate Results

The polycarbonate samples were measured utilizing the in-plane measurement technique. These samples were fabricated via nScrypt microdispensing. The S11 and S12 parameters of the transmission line samples were recorded and plotted based on their type of print. The first set of samples were designed with the DuPont 7082 sandwiched within the substrate. The data of these samples had a slight overlap and was inconsistent with what was expected with increasing volume fraction of DuPont 7082, which was due to the DuPont 7082 not being centered within the sample for each sample, as was discussed in chapter 3 and seen in Table 3.1. This caused sample 1 to have more loss than sample 2 and this is why sample 3 and 4 were very close to one

another. The S12 data for these samples can be seen in Fig. 4.10. The S11 data for these samples can be seen in Fig.4.11.

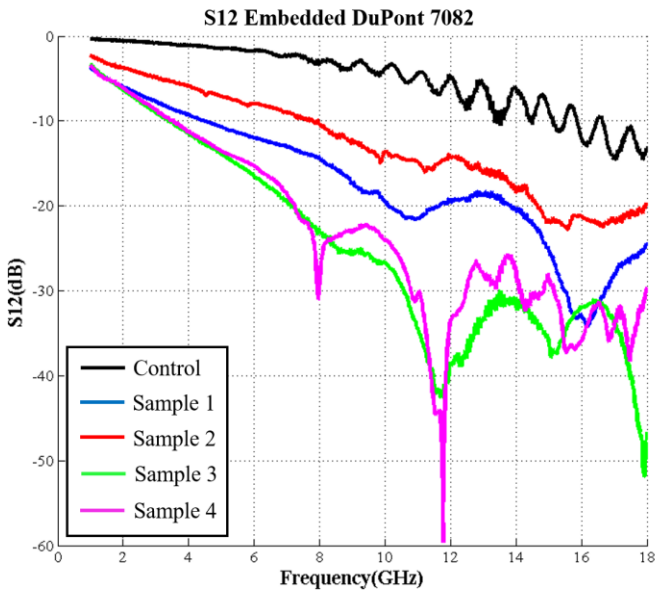

Figure 4.10 S12 plot for nScrypt printed transmission line samples with DuPont 7082 embedded within the substrate.

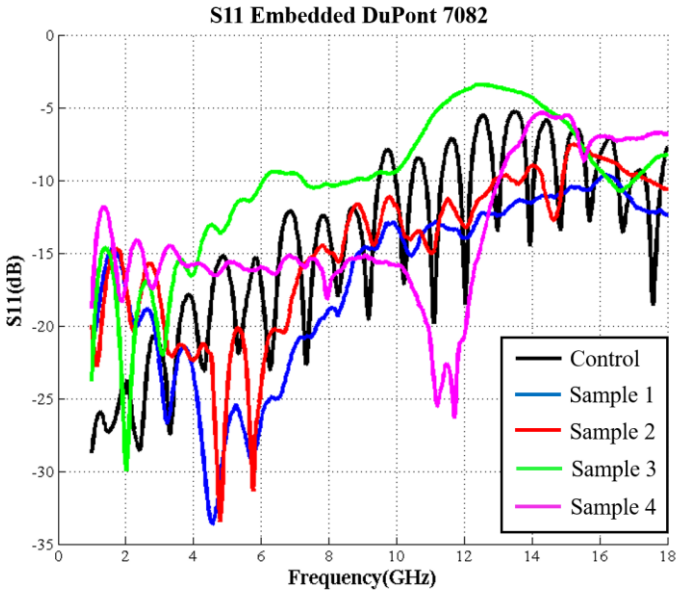

Figure 4.11 S11 plot for nScrypt printed transmission line samples with DuPont 7082 embedded within the substrate.

The second set of samples were designed with the DuPont 7082 printed at the surface of the substrate. The data of these samples had an increasing loss associated with increasing amounts of DuPont 7082 and provided more loss than the DuPont 7082 embedded samples, over a shorter distance. The structure and dimensions of these samples was discussed in chapter 3. The S12 data for these samples can be seen in Fig. 4.12. The S11 data for these samples can be seen in Fig.4.13.

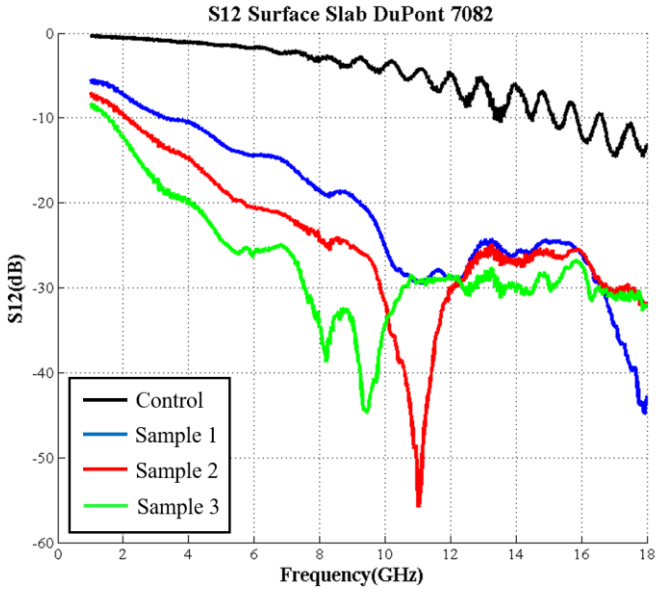

Figure 4.12 S12 plot for nScrypt printed transmission line samples with DuPont 7082 slab printed at the surface of the substrate.

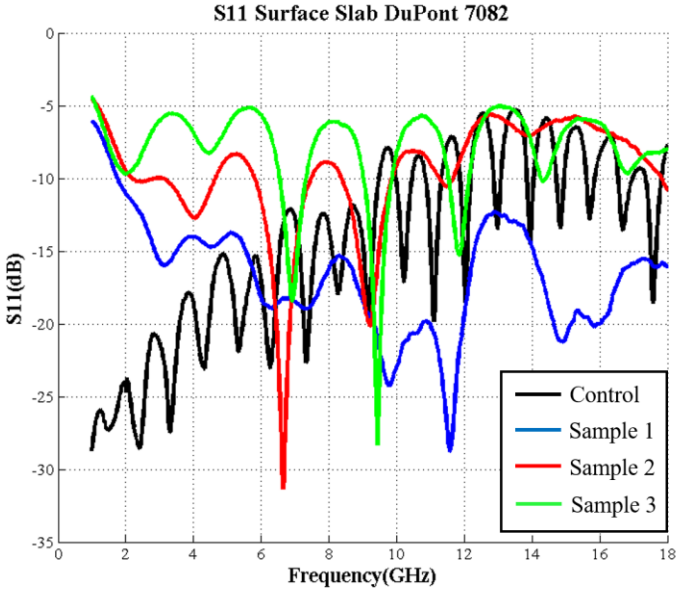

Figure 4.13 S11 plot for nScrypt printed transmission line samples with DuPont 7082 slab printed at the surface of the substrate.

The final sample was designed to combine the surface slabs of DuPont 7082 to create an optimized amount of loss with steps. The idea was to increase the amount of DuPont 7082 with steps, the structure and dimensions of this sample was discussed in chapter 3. The S12 and S11 data of the sample can be seen in Fig. 4.14 and 4.15.

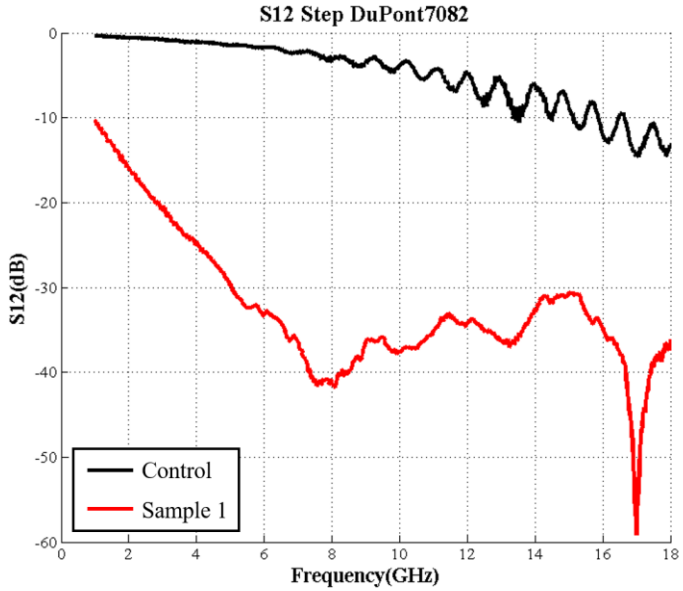

Figure 4.14 S12 plot for nScrypt printed transmission line sample with DuPont 7082 steps printed at the surface of the substrate.

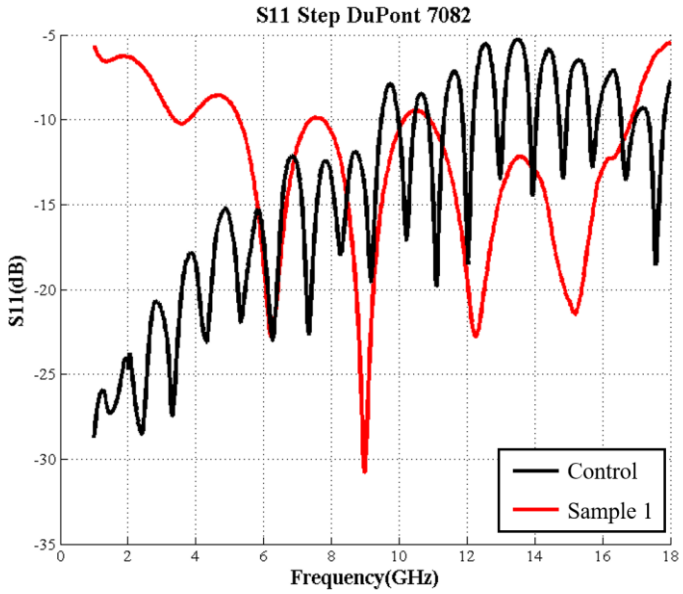

Figure 4.15 S11 plot for nScrypt printed transmission line sample with DuPont 7082 steps printed at the surface of the substrate.

4.3 Measurement and Characterization Conclusions

The fabricated in-plane and out of plane RF absorbers were measured and their results showed that there was an increase in transmission loss as the amount of DuPont 7082 was increased. The out of plane samples provided a small amount of transmission loss with only one sample, but if these samples were designed and processed to be made into a structural composite; these out of plane losses could be embedded within a structure and an increase in loss would be seen as the number of samples were stacked to create the composite [12, 17]. The in-plane absorbers showed that if the DuPont 7082 is placed at the surface of the substrate and the amount of DuPont 7082 is increased that the transmission losses increase. The high amount of transmission losses provide losses that could be used in antenna isolation and surface wave absorption.

Chapter 5

NUMERICAL MODELING

In this chapter, I will discuss the numerical modeling that was used in backing out the properties of the DuPont 7082. There were three types of software suites that were utilized for modeling. The first was Math Works MATLAB, which was utilized for reading results, plotting data, and modeling the out of plane characteristics of the DuPont 7082. The second was Ansys HFSS, which was utilized in the modeling of the in-plane samples and aided in the fabrication of the in-plane absorbers. And the third was COMSOL, which was used in the modeling of the cross section of the transmission lines to determine that index of refraction based on the location of the embedded DuPont 7082. The methods and characterization processes that were implemented are described below.

5.1 MATLAB Modeling

MATLAB was utilized to read results, plot data, and model the out of plane characteristics of the fabricated structures. In order to model the characteristics of the DuPont 7082, MATLAB was first used to read in the transmission data that was recorded from the network analyzer. The data was placed into column vectors, so that it could be easily plotted and manipulated.

The measured Kapton transmission data and confocal data was used in backing out the material properties of the DuPont 7082 through the use of rigorous coupled wave analysis. The rigorous coupled wave analysis that was used is a computational method used to calculate the complex transmission and reflection characteristics of a periodic dielectric structure. This analysis was used in this research to optimize the permittivity of the DuPont to match the transmission data that was recorded from the Kapton printed

samples. An optimized complex permittivity was determined through the use of the Debye equation [29]:

$$\varepsilon_r(\omega) = \varepsilon_r'(\omega) - j\varepsilon_r''(\omega) = \varepsilon_{r\infty}' + \frac{\varepsilon_{rs}' - \varepsilon_{r\infty}'}{1+j\omega\tau_e} \tag{5.1}$$

The program read in the transmission data from the parallel and perpendicular polarizations of the samples, the index of refraction of the materials used, an estimated value of the permittivity of the DuPont 7082, the frequency used, the period of the structure, the width of the printed lines, and the thickness of the printed lines. The program then utilizes these variables and rigorous coupled wave analysis to calculate a Debye fit of the complex permittivity, the results are plotted in Fig. 5.1. The frequencies that were not measured for the Kapton were plotted based on the Debye equation.

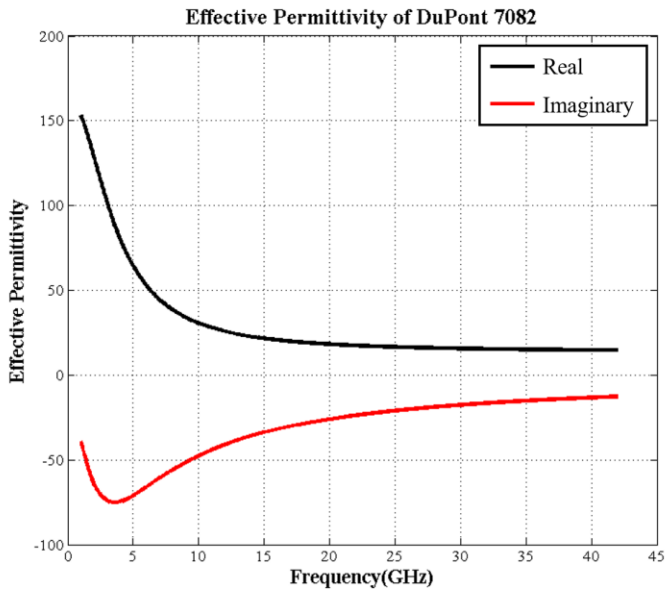

Figure 5.1 Effective permittivity of DuPont 7082 based on rigorous coupled wave analysis and the Debye equation.

The data that was produced for the complex permittivity of the DuPont 7082 was then used to plot the frequency dependence of the relative permittivity and the loss tangent, plotted in Fig.5.2. This material information was necessary in the modeling of the structures in HFSS.

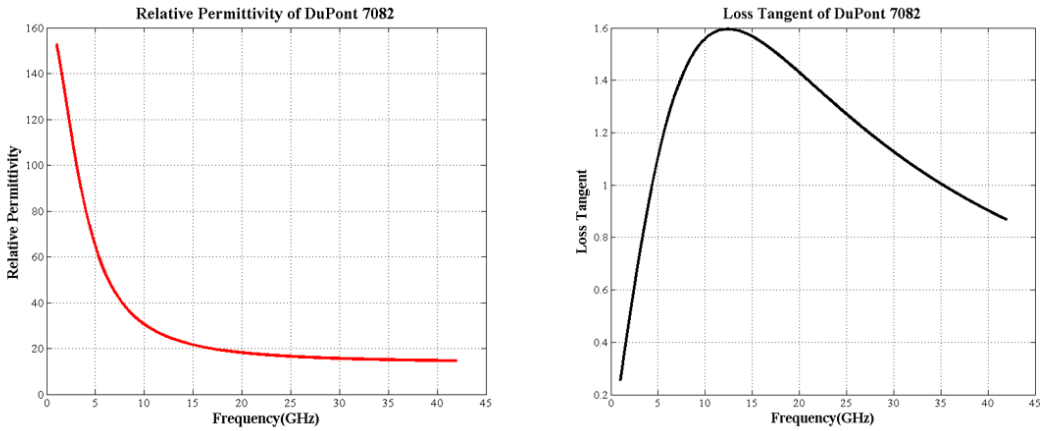

Figure 5.2 Relative permittivity of DuPont 7082 (left) and loss tangent of DuPont 7082 (right).

5.2 HFSS Modeling

HFSS was utilized in the modeling and simulation of the in-plane samples. These samples were designed to determine the effectiveness of the DuPont 7082 ink in the use of in-plane absorption. The first step of the simulations was to determine the design criteria of the transmission lines. The transmission line was initially designed to be used at 8GHz. At this frequency, the baseline transmission line was designed. Because the baseline transmission line would contain only polycarbonate, the relative permittivity of the substrate would be 2.9 [3]. The width used was 25mm, the desired height was 1.2 mm. The length of the TL was decided to be 100.75 mm. This allowed

for a quarter wavelength gap to occur before and after the DuPont 7082. This was designed to allow the wave to couple to the line before the DuPont 7082 would interfere. The final parameter that was used in the calculation of the input impedance was the trace width. The trace width was decided to be 3.1mm in order to closely match a 50 ohm input impedance. The SMA connectors used were designed to be 50 ohms.

The next step was to create simulations for a transmission line with a DuPont 7082 slab placed within the center of the substrate, as discussed in Chapter 3 and seen in Fig.3.8. The carbon thickness was centered within the substrate, and the thickness of DuPont 7082 was varied. These simulations produced a noticeable loss when compared to the baseline, the S12 and S11 simulation results can be seen in Fig. 5.3 and Fig. 5.4. It was initially thought that the transmission loss would be dependent upon the volume fraction of DuPont 7082 to polycarbonate within the substrate. However, when creating the fabricated samples, the DuPont 7082 was not able to be centered, due to the thickness of the lines that were printed by the nScrypt. This required that the printed DuPont 7082 slab be printed closer to the trace of the transmission line, as discussed in chapter 3. This shift up from being centered created a loss that did not match the initial simulation results for the centered samples. A new simulation that factored in the shift of the slab was completed and this confirmed that the loss was not only a function of the volume fraction of DuPont 7082, but that the loss was also location dependent.

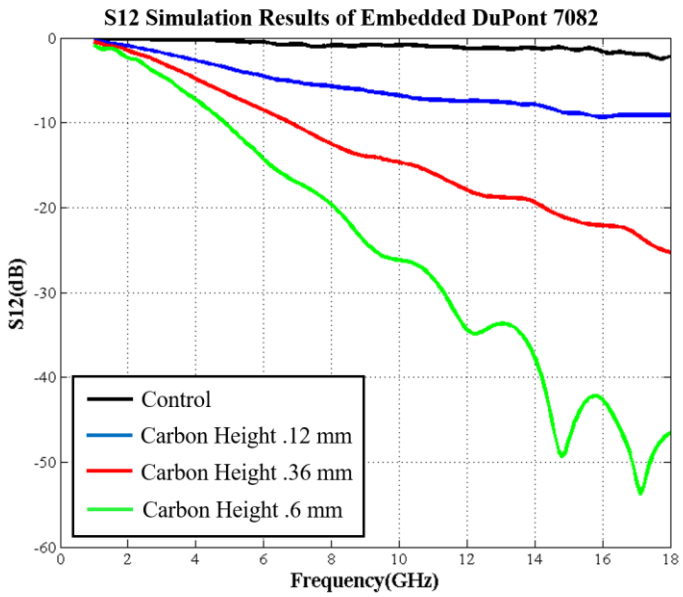

Figure 5.3 S12 plot of simulated transmission line samples with DuPont 7082 slab embedded within the substrate. The carbon height is the thickness of the carbon that is centered within a 1.2 mm thick substrate.

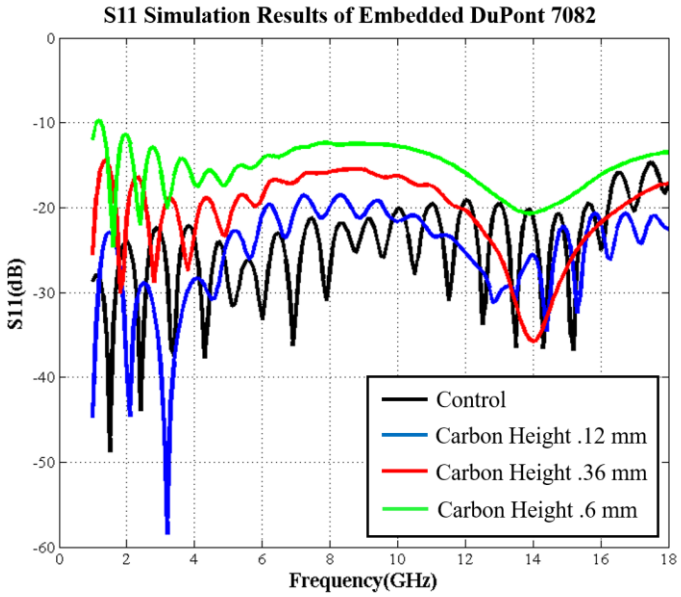

Figure 5.4 S11 plot of simulated transmission line samples with DuPont 7082 slab embedded within the substrate. The carbon height is the thickness of the carbon that is centered within a 1.2 mm thick substrate.

As was seen with the measured samples, shifting the DuPont 7082 slab location closer to or farther from the surface of the substrate, the amount of loss was dependent upon the location of the DuPont 7082 slab within the substrate. Upon closer inspection, it was demonstrated that as the DuPont 7082 is placed closer to the top surface of the substrate that the loss increases, and that the loss was at a maximum when the carbon was placed at the surface of the substrate; this was confirmed with simulations in COMSOL. Simulations of the substrate with the DuPont 7082 at the surface were completed and measurements were taken. For these samples, the printed DuPont 7082 slab was located at the surface of the substrate and projected down into the substrate with varying thicknesses. As the thickness was increased, the loss also increased, the S12 and S11 are plotted in Fig.5.5 and Fig. 5.6.

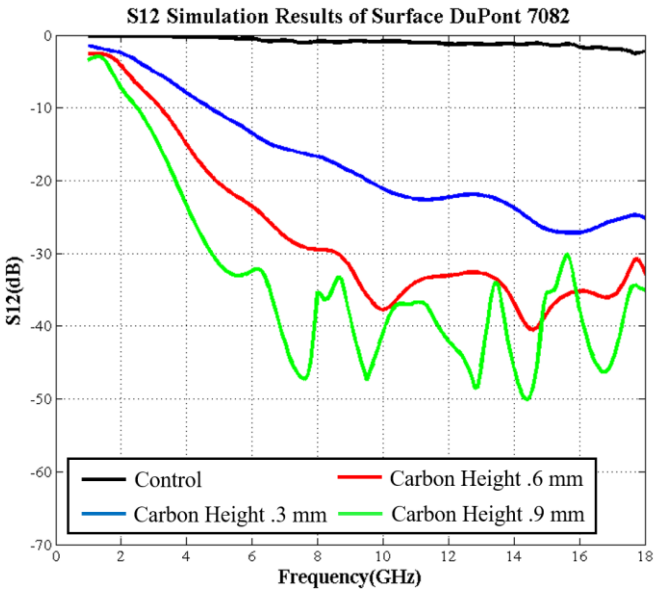

Figure 5.5 S12 plot of simulated transmission line samples with DuPont 7082 slab located at the surface of the substrate. The carbon height is the thickness of the carbon that is located at the surface of a 1.2 mm thick substrate.

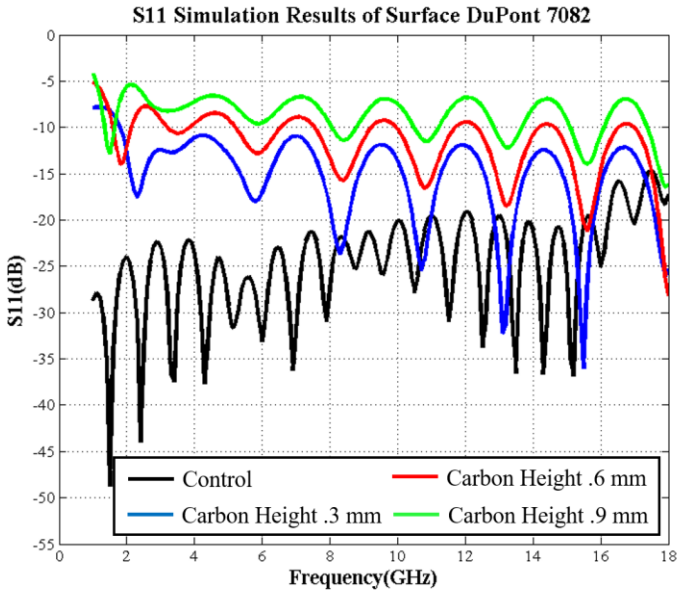

Figure 5.6 S11 plot of simulated transmission line samples with DuPont 7082 slab located at the surface of the substrate. The carbon height is the thickness of the carbon that is located at the surface of a 1.2 mm thick substrate.

The results from the slab located near the surface of the transmission line substrate produced desirable losses; however, simulations were done to try and optimize the losses. By creating a step function, as discussed in chapter 3 and seen in Fig.3.11, simulations showed that an increased loss could be attained. The S12 and S11 simulated results can be seen in the plot located in Fig. 5.7 and Fig. 5.8. These results show that the graded structure had a higher amount of in-plane loss and a better S11, when compared with the thickest surface slab.

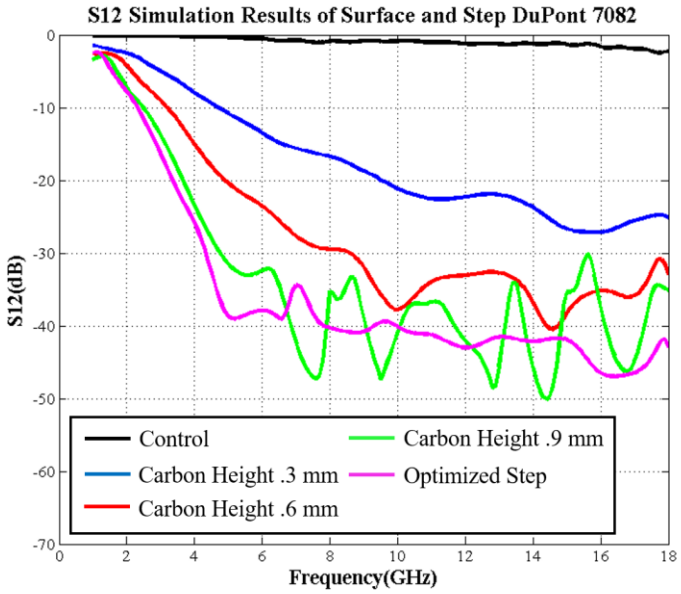

Figure 5.7 S12 plot of simulated transmission line samples with DuPont 7082 slab located at the surface of the substrate and optimized step slab.

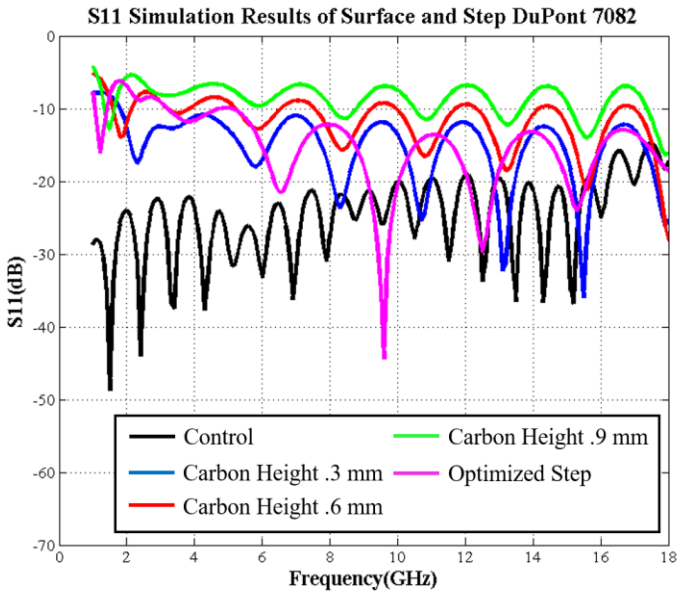

Figure 5.8 S11 plot of simulated transmission line samples with DuPont 7082 slab located at the surface of the substrate and optimized step.

5.3 Modeling Conclusions

Numerical modeling techniques have provided a solution to determining the complex permittivity of DuPont 7082. This permittivity was then used in the simulating of in-plane RF absorbing structures, which were then additively manufactured and measured. From these results, an optimized structure was created with ideal loss characteristics. The loss characteristics were designed to provide a high amount of transmission loss and to grade the structure to allow for a low amount of reflection at the interface of the polycarbonate substrate and the DuPont 7082. This optimized sample proves that DuPont 7082 can act as a lossy material in the used of in-plane RF absorbers. Based on the results of the out of plane measurements of DuPont 7082, if this material was to be printed on to multiple substrates and embedded within a stack of composite sheets, a structural composite with integrated out of plane loss could be created. The comparison of the measured and simulated results of the optimized step structure can be seen in Fig.5.9 and Fig. 5.10.

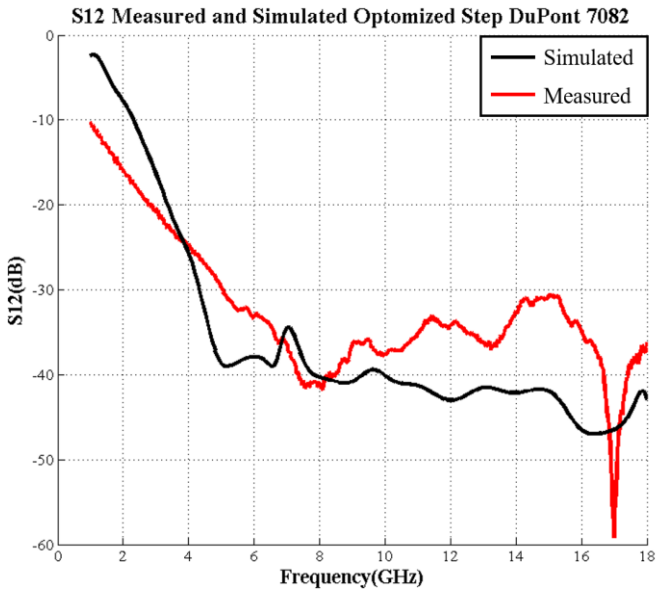

Figure 5.9 Plot of measured and simulated S12 of the optimized step DuPont 7082 in-plane absorber.

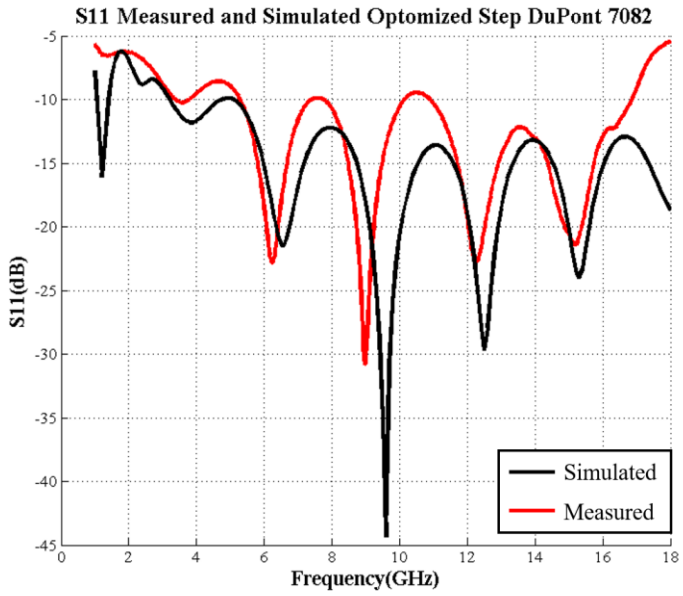

Figure 5.10 Plot of measured and simulated S11 of the optimized step DuPont 7082 in-plane absorber.

Chapter 6

CONCLUSIONS AND FUTURE WORK

6.1 Conclusion

Through the research that was complete in this thesis, samples were fabricated utilizing both screen printing and nScrypt microdispensing. Screen printing was primarily used to create large scale out of plane RF absorbers. This printing technique allows the user to combined RF absorption characteristics with composite sheets, which can then be used in the fabrication of structures. nScrypt microdispensing was used in the fabrication of small scale in-plane and out of plane RF absorbers. Through this printing technique, samples were fabricated that utilized transmission line design to create in-plane absorbers and accurately deposited line structures to create out of plane absorbers that were used to characterize DuPont 7082

The fabricated in-plane and out of plane RF absorbers were measured and their results showed that there was an increase in transmission loss as the amount of DuPont 7082 within a sample was increased. The out of plane samples provided a small amount of transmission loss with only one sample, but if these samples were designed and processed to be made into a structural composite; these out of plane losses could be embedded within a structure and an increase in loss would be seen as the number of samples were stacked to create the composite. The in-plane absorbers showed that if the DuPont 7082 is placed at the surface of the substrate and the amount of DuPont 7082 is increased that the transmission losses increase. The high amount of transmission losses provide losses that could be used in antenna isolation and surface wave absorption.

Numerical modeling techniques have provided a solution to determining the complex permittivity of DuPont 7082. This permittivity was then used in the simulating of in-plane RF absorbing structures, which were then additively manufactured and measured. From these results, an optimized structure was created with ideal loss characteristics. The loss characteristics were designed to provide a high amount of transmission loss and to grade the structure to allow for a low amount of reflection at the interface of the polycarbonate substrate and the DuPont 7082. This optimized sample proves that DuPont 7082 can act as a high loss material in the used of in-plane RF absorbers. Also, based on the results of the out of plane measurements of DuPont 7082, if this material was to be printed on to multiple substrates and embedded within a stack of composite sheets, a structural composite with integrated out of plane loss could be created.

6.2 Future Work

The results from this research have shown that through the use of additive manufacturing, RF absorbing characteristics can be combined with composite fabrics and films and that these characteristics can be embedded within the substrate of microstrip lines to cause transmission losses with low amounts of reflections. The next step of this research is to apply the results to real world applications. The applications in which DuPont 7082 would could to as a solution are antenna isolation [24] and surface wave absorption [18-20, 25-27]. This could be attempted by multiple methods. One method to apply to antenna isolation would be to print DuPont 7082 onto composite sheets and to uses these sheets when creating an array of antenna structures to eliminate interference between composite integrated antennas. Another, would be to create the antenna substrate through the use of an nScrypt and to place a graded absorber between

the antennas within the array. The other application in which DuPont 7082 could be used is to reduce the radar cross section of a metal sheet. This can be made possible by adding edge absorbers to absorb the surface waves that create the back scattering [29, 20, 25-27]. All of these methods could be used to apply the results of this research to a real world applications.

REFERENCES

1. P. Pa, M. Mirotznik, and S. Yarlaggada, "High Frequency Characterization of Conductive Inks Embedded within a Structural Composite," *2015 IEEE International Symposium on Antennas and Propagation & USNC/URSI National Radio Science Meeting*, pp. 1310-1311, 2015.

2. P. Pa, Z. Larimore, P. Parsons, and M. Mirotznik, "Multi-material additive manufacturing of embedded low-profile antennas," *Electronics Letters*, vol. 51, no. 20, pp. 1561-1562, 2015.

3. P. Pa, *Additive Manufacturing of Electromagnetic Multifunctional Composites*, Newark, DE: Dissertation, University of Delaware, 2015.\

4. R. McCauley, *Material Design Methodology for Structural and Microwave Multifunctional Composite Laminate Systems*, Newark, DE: Master's Thesis, University of Delaware, 2013

5. F. Qin and C. Brosseau, "A review and analysis of microwave absorption in polymer composites filled with carbonaceous particles," *Journal of Applied Physics*, vol. 111, no. 061301, 2012.

6. J. Kim and J. Byun, "Salisbury Screen Absorbers of Dielectric Lossy Sheets of Carbon Nanocomposite Laminates," *IEEE Transactions on Electromagnetic Compatibility*, vol. 54, no. 1, pp. 37-42, 2012.

7. J. Oh, K, Oh, C. Kim, and C. Hong, "Design of radar absorbing structures using glass/epoxy composite containing carbon black in X-band frequency ranges," *Composites Part B-Engineering*, vol. 35, no. 1, pp. 45-56, 2004.

8. S. Lee, J. Kang, and C. Kim, "Fabrication and design of multi-layered radar absorbing structures of MWNT-filled glass/epoxy plain-weave composites," *Composite Structures*, vol. 76, no. 4, pp 397-405, 2006

9. D. Micheli, C. Apollo, R. Pastore, R. Morles, S. Laurenzi, and M. Marchetti, "Nanostructured composite materials for electromagnetic interference shielding applications," *Acta Astronautica*, vol. 69, no. 9-10, pp. 747-757, 2011.

10. W. Lee, J. Lee, and C. Kim, "Characteristics of an electromagnetic wave absorbing composite structure with a conducting polymer electromagnetic bandgap (EBG) in the X-Band," *Composites Sciences and Technology*, vol. 68, no. 12, pp. 2485-2489, 2008

11. A. Ashraf, M. Tariq, K. Naveed, A. Kausar, Z. Iqbal, Z. Khan, and L. Khan, "Design of Carbon/Glass/Epoxy-Based Radar Absorbing Composites: Microwaves Attenuation Properties," *Polymer Engineering and Science*, vol. 54, no. 11, pp. 2508-2514, 2014

12. I. Seo, W. Chin, and D. Lee, "Characterization of electromagnetic properties of polymeric composite materials with free space method," *Composite Structures*, vol.66, no. 1-4, pp. 533-542, 2004

13. K. Park, S. Lee, C. Kim, and J. Han, "Fabrication and electromagnetic characteristics of electromagnetic wave absorbing sandwich structures," *Composites Science and Technology*, vol. 66, no. 3-4, pp. 576-584, 2006.

14. H. Baskey, M. Akhtar, and T. Shami, "Investigation and performance evaluation of carbon black-and carbon bibers-based wideband dielectric absorbers for X-band stealth applications," *Journal of Electromagnetic Waves and Applications*, vol. 28, no.14, pp. 1703-1715, 2014.

15. M. Achour, M. Malhi, J. Miane, F. Carmona, and F. Lahjomri, "Microwave properties of carbon black-epoxy resin composites and their simulation by means of mixture laws," *Journal of Applied Polymer Science*, vol. 73, no. 6, pp. 969-973, 1999

16. D. Micheli, C. Apollo, R. Pastore, and M. Marchetti, "X-Band microwave characterization of carbon-based nanocomposite material, absorption capability comparison and RAS design simulation," *Composites Science and Technology*, vol. 70 no. 2 pp. 400-409, 2010.

17. D. Micheli, A Vricella, R. Pastore, and M. Marchetti, "Synthesis and electromagnetic characterization of frequency selective radar absorbing materials using carbon nanopowders," *Carbon*, vol. 77, pp. 756-774, 2014.

18. N. Das, D. Khastgir, T. Chaki, and A. Chakraborty, "Electromagnetic interference shielding effectiveness of carbon black and carbon fibre filled EVA and NR based composites," *Composites Part A-Applied Science and Manufacturing*, vol. 31, no.10, pp. 1069-1081, 2000.

19. H. Chen, L. Lu, D. Guo, H. Lu, P. Zhou, J. Xie, and L. Deng, "Relationships between Surface Wave Attenuation and the Reflection Properties of Thin Surface Wave Absorbing Layer," *PIERS Proceedings*, pp. 1146-1150, 2014

20. F. Smith, "Edge coatings that reduce monostatic RCS," *IEE Proceedings-Radar Sonar and Navigation*, vol. 149, no. 6, pp. 310-314, 2002.

21. F. Costa, A. Monorchio, and G. Manara, “Analysis and Design of Ultra-Thin Electromagnetic Absorbers Comprising Resistively Loaded High Impedance Surfaces,” *IEEE Transactions on Antennas and Propagation*, vol. 58, no5, 2010.

22. J. Yang and Z. Shen, “A Thin and Broadband Absorber Using Double-Square Loops,” *IEEE Antennas and Wireless Propagation Letters*, vol. 6, pp. 388 – 391, 2007

23. L. Hai-Tao, C. Hai-Feng, C. Zeng-Yong, Z. De-Yong, “Absorbing properties of frequency selective surface absorbers with cross-shaped resistive patches,” *Materials and Design*, vol. 28, no. 7, pp.2166-2171, 2007

24. A. Abdelaziz, “Improving the Performance of an Antenna Array by Using Radar Absorbing Cover,” *Progress in Electromagnetic Research Letters*, vol. 1, pp. 129-138, 2008.

25. H. Chen, P. Zhou, L. Chen, and L. Deng, “Study on the Properties of Surface Waves in Coated RAM Layers and Mono-static RCSR Performances of a Coated Slab,” *Progress in Electromagnetic Research M*, vol. 11, pp. 123-135, 2010.

26. H. Chen, J. Xie, Z. Zhu, and L. Deng, “Method of Tapered Resistive Sheet Loading for Controlling Edge Scattering,” *Microwave and Optical Technology Letters*, vol. 55, no. 9, pp. 1992-1996, 2013.

27. H. Chen, Z. Zhu, L. Lu, Y. Gaun, J. Xie, and L. Deng, “Design and implementation of the tapered resistive sheets to control edge scattering,” *Journal of Applied Physics*, vol. 115, no. 164906, 2014.

28. D. Pozar, *Microwave Engineering*, Hoboken, NJ: John Wiley & Sons, Inc., 2005

29. C.A. Balanis, *Advanced Engineering Electromagnetics*, John Wiley and Sons, 1989.

30. M. Radmanesh, *Radio Frequency and Microwave Electronics*, Prentice Hall, 2001